DETERMINATION OF ELECTROCHEMICAL PERFORMANCE, AND THERMO-MECHANICAL-CHEMICAL STABILITY OF SOFCS FROM DEFECT MODELING

Eric D. Wachsman, Keith L. Duncan and Fereshteh Ebrahimi
Department of Materials Science
University of Florida, Gainesville FL 32611

Department of Energy, Contract Number DE-FC26-02NT41562

OBJECTIVES

1. Provide fundamental relationships between SOFC performance and operating conditions (T, P_{O_2}, V, etc..)
2. Transient (time dependent) transport properties
3. Extend models to:
   - Thermo-mechanical stability
     - Thermal and thermochemical expansion
     - Elastic modulus
     - Fracture toughness
   - Thermo-chemical stability
     - Pore formation and reactions at cathode/electrolyte interface
   - Multilayer structures
     - Interfacial defect concentration, etc.
4. Incorporate microstructural effects such as grain boundaries and grain-size distribution
5. Experimentally verify models and devise strategies to obtain relevant material constants
6. Assemble software package for integration into SECA failure analysis models

CONTINUUM LEVEL ELECTROCHEMICAL MODEL - Phase 1

Features of the Defect Model

- Continuous functions for the defect concentrations vs. discontinuous "piecewise" Brouwer approach
- Dependent on thermodynamic quantities, namely the mass-action constants (K's)
- Derived from fundamental thermodynamic equations
- Quantitative for any ceramic SOFC material.

Electron-Hole Pair Formation

$$null \leftrightarrow e' + h^{\bullet}$$

$$K_i = c_e c_h = N_v N_c \exp\left(-E_g / k_B T\right)$$

External Equilibria

$$O_O^{\times} \leftrightarrow V_O^{\bullet\bullet} + 2e' + \frac{1}{2} O_2$$

$$K_r = c_V c_e^2 P_{O_2}^{\frac{1}{2}} = K_r^* \exp\left(-\Delta G_r / k_B T\right)$$

Internal Equilibria

$$O_O^{\times} \leftrightarrow V_O^{\bullet\bullet} + O_i''$$

$$K_f = c_V c_I$$

Defect Triads (CLEM)	vs.	Defect Pairs (Brouwer)
$c_e + c_A = 2c_V$		$c_e = 2c_V$ …Region I
Limiting Case		$c_A = 2c_V$ …Region IIa
$P_{O_2} >> 4^{-4} K_r^2 c_V^{-6}$		

CONTINUUM LEVEL ELECTROCHEMICAL MODEL - Phase 1

FLUORITE

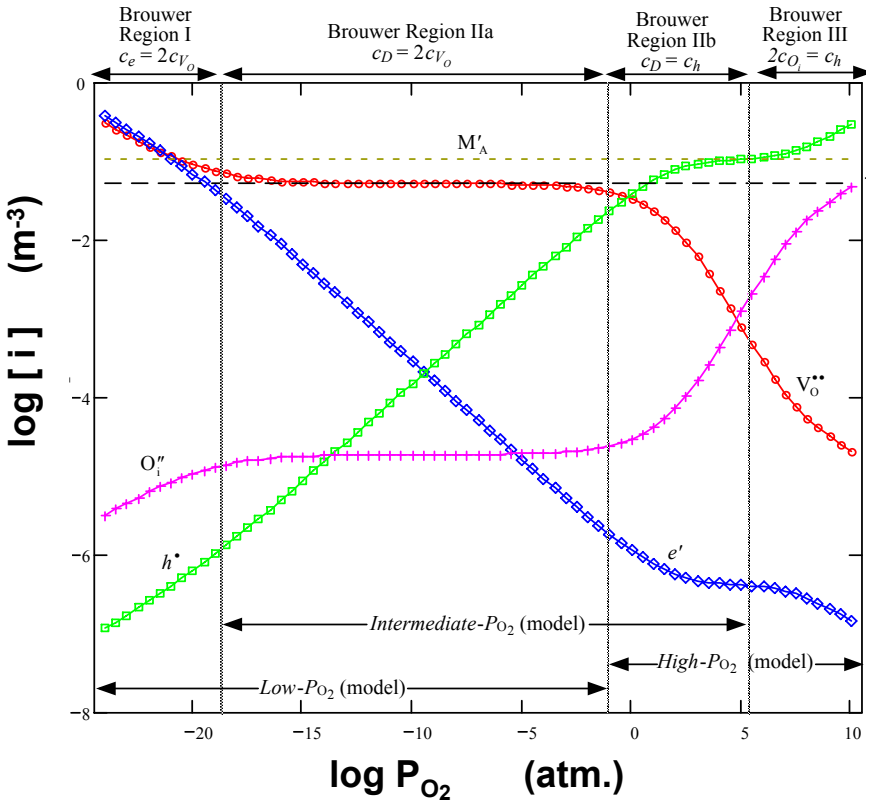

PEROVSKITE

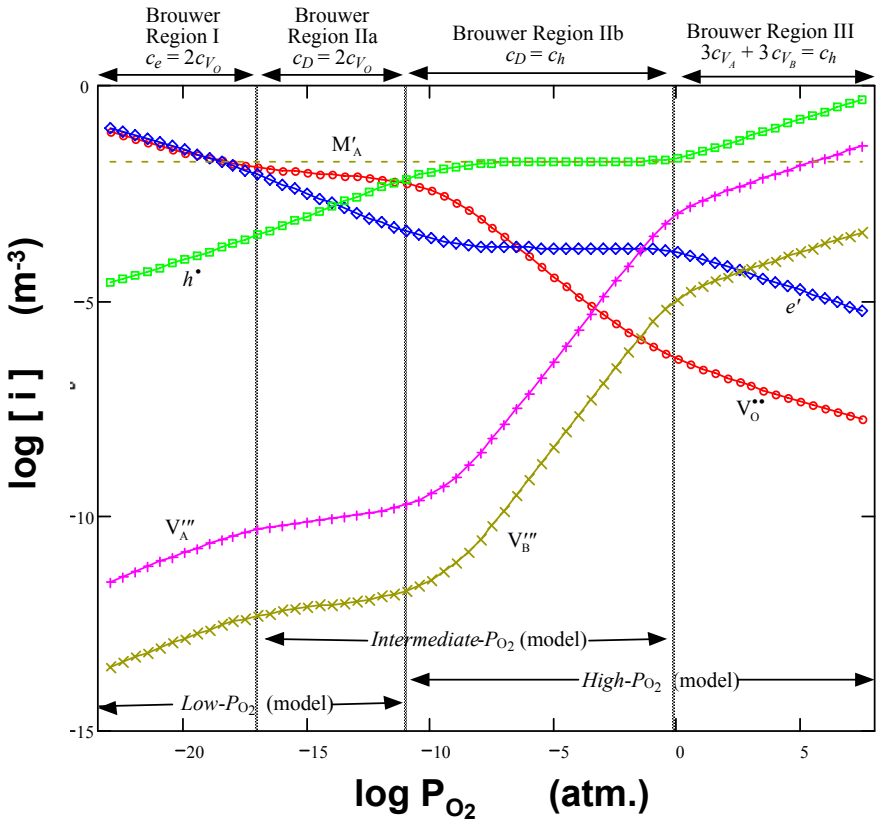

Verified experimentally

- vs. other models[1]
- vs. conductivity[2]
- vs. OCP

1. O. Porat and H. L. Tuller, *J. Electroceramics* **1** (1997) 42; 2. Eguchi et al, *Solid State Ionics* **52** (1992) 265.

DEMONSTRATION OF CLEM SOFTWARE PACKAGE

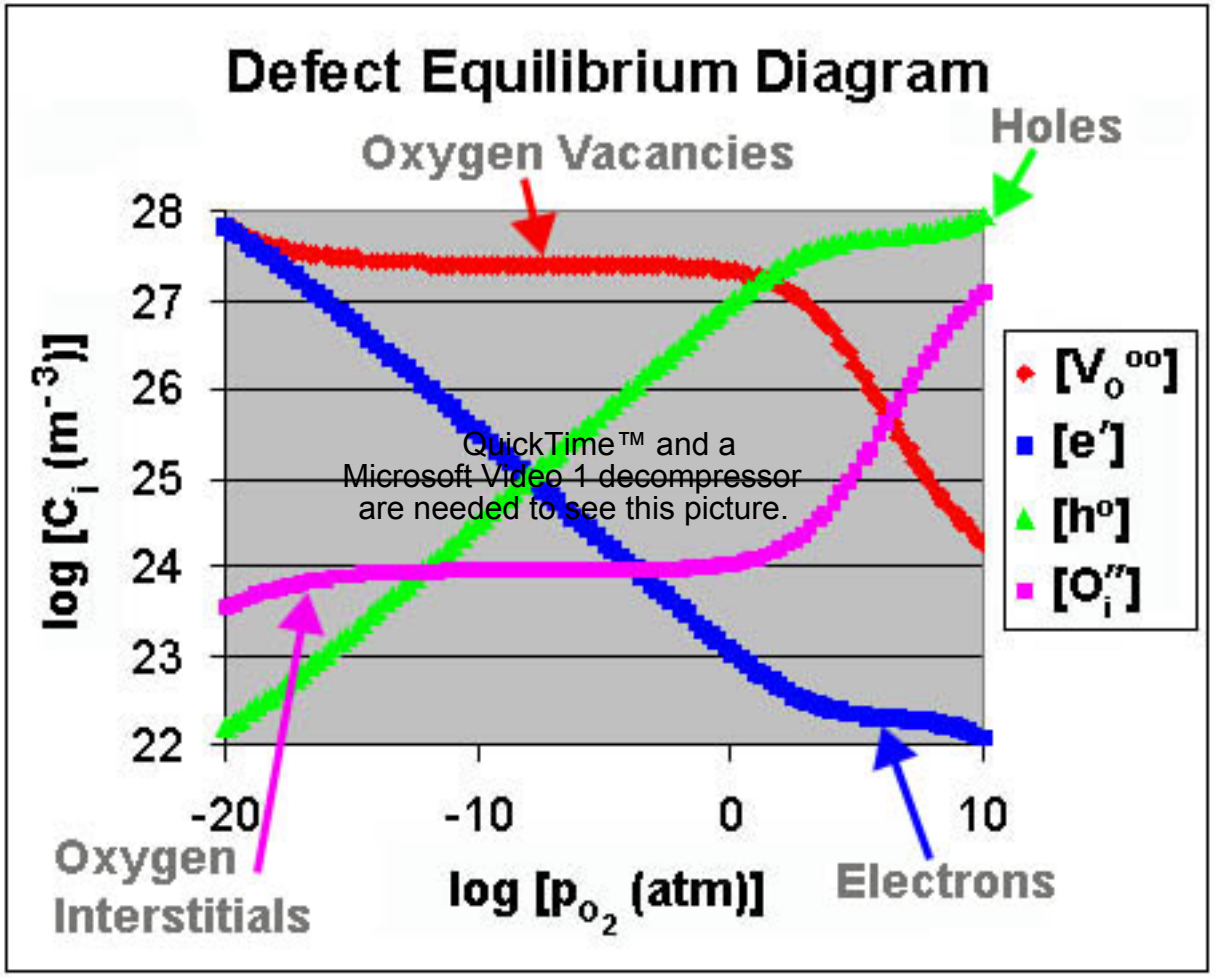

Multiplatform C++ program
Available at www.mse.ufl.edu/~ewach

CONTINUUM LEVEL ELECTROCHEMICAL MODEL - Phase 1

FLUORITE

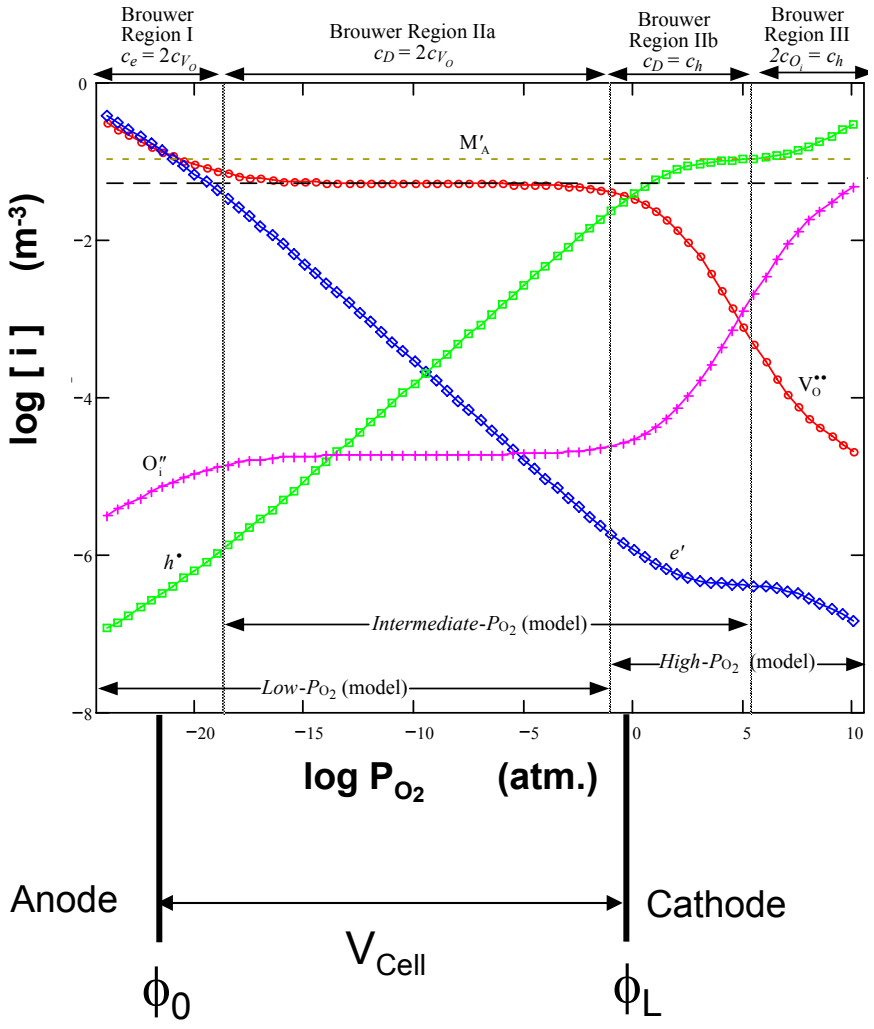

Electrochemical Performance

Provides relationship between defect concentration and voltage

$V_{Cell} = \phi_L - \phi_L = V_{OC} - J \bullet \Sigma R_i$

$R_i \sim 1 / [i]$

$$\phi(x) = \phi_0 - \frac{(D_V\gamma - j_V)k_BT}{z_V q D_V \gamma} \cdot \ln \frac{z_V(z_V - z_e)D_V\gamma c_V(x) - j_V c_A}{z_V(z_V - z_e)D_V\gamma c_{V_0} - j_V c_A}$$

$$j_V = -\frac{(z_V - z_e)qD_eD_V\gamma}{k_BT}\left[u_e - u_V \frac{z_V}{z_e^2}\left(\frac{1}{\bar{t}_{ion}} - 1\right)\left(\frac{k_BT\ln(c_{e_L}/c_{e_0}) + z_e q\Delta\phi}{k_BT\ln(c_{V_L}/c_{V_0}) + z_V q\Delta\phi}\right)\right]^{-1}$$

$$j_e = j_V \frac{z_V^2}{z_e^2}\left(\frac{1}{\bar{t}_{ion}} - 1\right)\left(\frac{k_BT\ln(c_{e_L}/c_{e_0}) + z_e q\Delta\phi}{k_BT\ln(c_{V_L}/c_{V_0}) + z_V q\Delta\phi}\right)$$

Removed linear potential and fixed boundary assumptions typically used

CONTINUUM LEVEL ELECTROCHEMICAL MODEL - Phase 1

FLUORITE

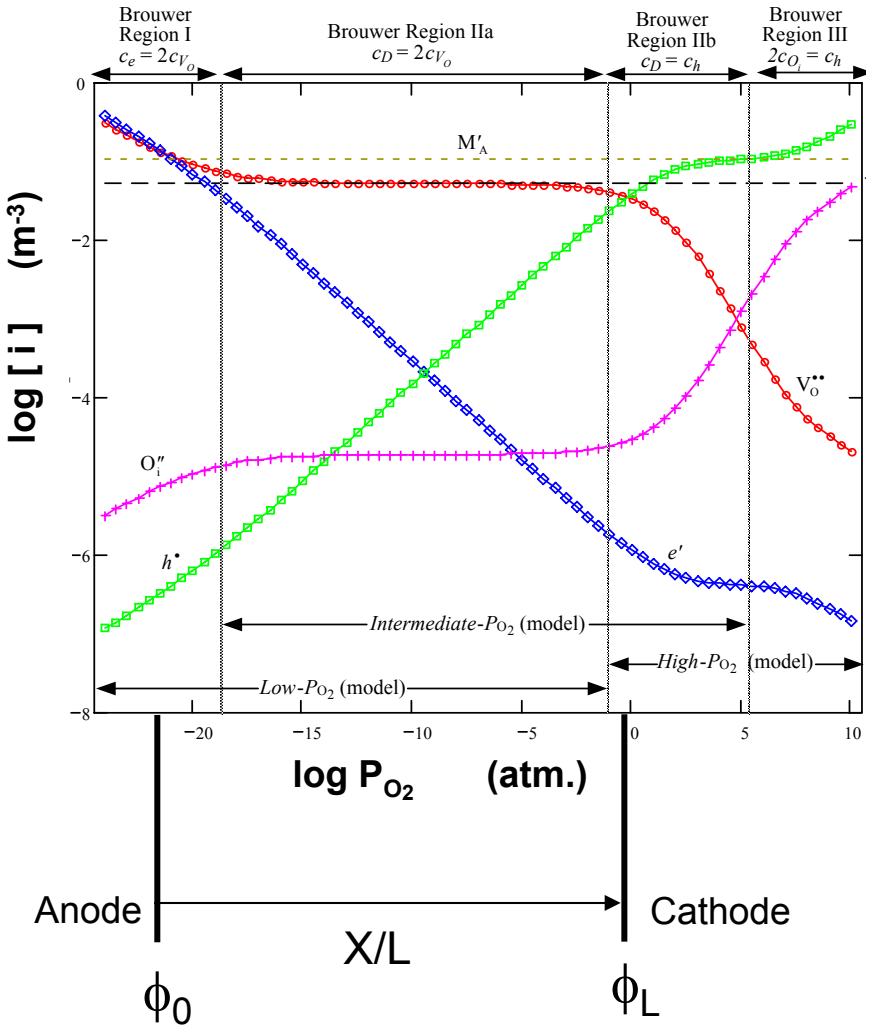

Spatial Distribution

Provides defect concentration as a function of position (X) in the cell

$$c_V(x) - c_{V_0} - \frac{(D_V\gamma - j_V)c_A}{z_V(z_V - z_e)D_V\gamma} \cdot \ln\frac{z_V(z_V - z_e)D_V\gamma c_V(x) - j_V c_A}{z_V(z_V - z_e)D_V\gamma c_{V_0} - j_V c_A} = -\gamma x$$

$$\gamma = \frac{\phi_L - \phi_0}{\lambda L} - \frac{c_{V_L} - c_{V_0}}{L} \qquad \lambda = \frac{(z_V - z_e)k_B T}{z_e q c_A}$$

-> Thermo-chemical Stability

-> Thermo-mechanical Stability

TASKS TO BE PERFORMED IN PHASE 2

1. Extend Continuum Level Electrochemical Model to Include Multi-Layer Structures

Determine effects of component thickness ratios and operating conditions on the concentration of defect species and oxygen potential at component interfaces.

2. Extend Continuum Level Electrochemical Model to Include Microstructural Effects

Determine effects of microstructure on the electrical, thermo-mechanical and thermo-chemical stability of SOFC components and SOFC performance.

3. Experimentally Verify Thermo-Mechanical Model

Measure oxygen stoichiometry (Cahn Microbalance) and material expansion (Theta Dilatometer) as a function of P_{O_2} & T. Measure modulus and fracture toughness of single crystal regions as a function of P_{O_2} & T (Triboindenter). Measure modulus and fracture toughness of polycrystalline samples (MTS system) and separate bulk property vs. microstructural effects. Compare with data obtained at ORNL.

4. Verify Electrochemical Performance , Chemical Stability, and Transient Aspects of Model

Obtain frequency dependent impedance and electrode overpotential data from electrochemical measurements (ac impedance spectroscopy, potentiometric, current interrupt, etc,) to determine effects of porosity and pore diffusion (electrodes); grain boundaries (electrolyte); and grain-size distribution.

Induce degradation/failure in cathode/electrolyte bilayers by thermal cycling, high temperature sintering and DC bias to initiate tertiary phase formation or delamination at the interface. Experimentally determine cell time constants from R-C circuit analysis and use in evaluating the effect of voltage transients from the power conditioning equipment on failure mechanisms.

5. Package and Deliver Software

Develop software modules of the models for use by NETL, PNNL, ORNL and SECA industrial teams.

PHASE 2 SCHEDULE - Gant Chart

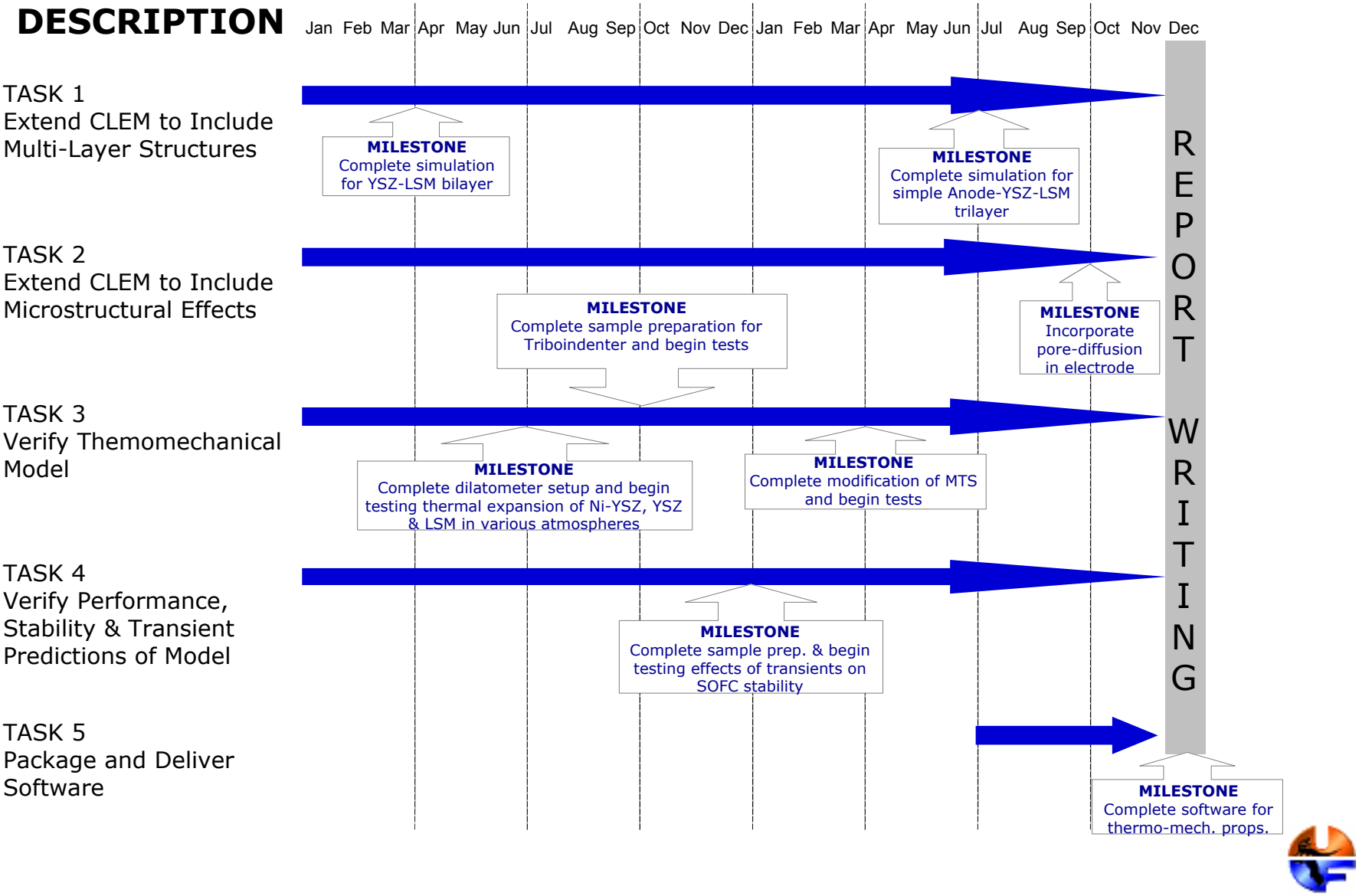

EXTENDING CONTINUUM LEVEL ELECTROCHEMICAL MODEL MODEL TO MULTILAYERED SOFC ARCHITECTURE

Present Approach

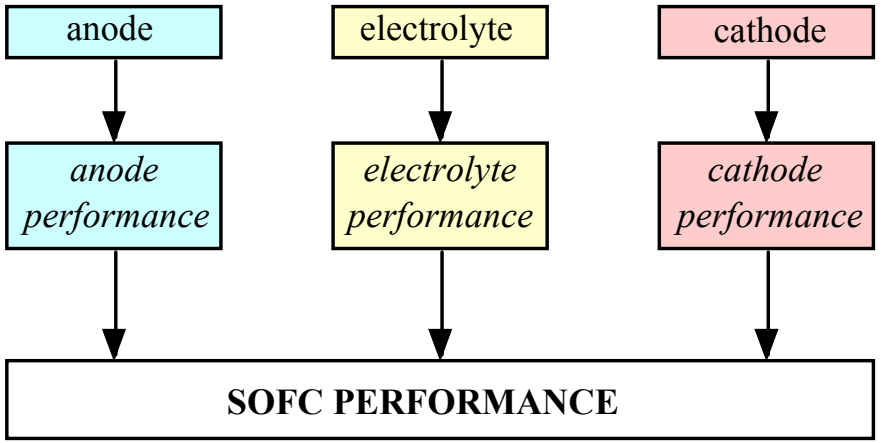

Proposed Approach

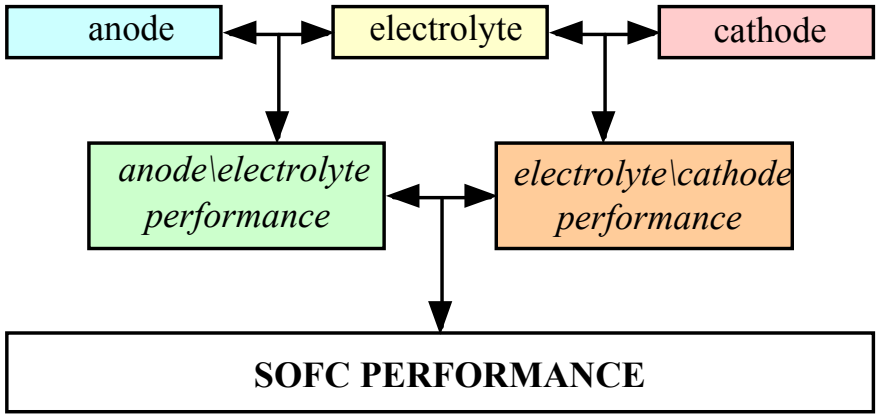

Cathode Supported

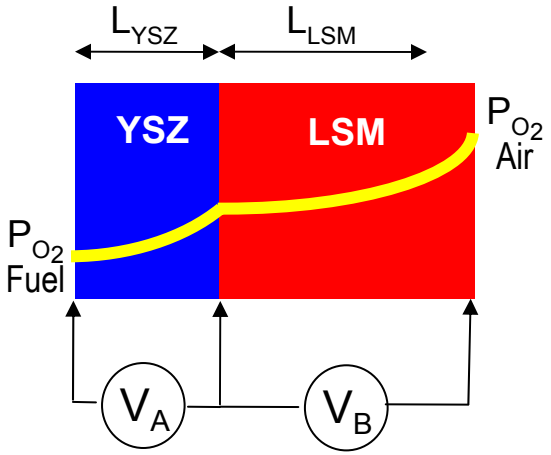

Anode or Electrolyte Supported

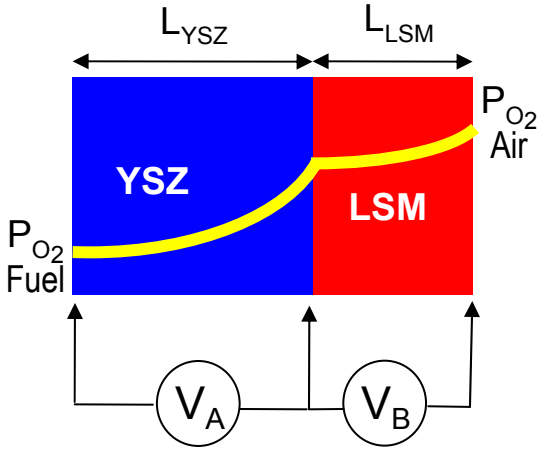

$V_A + V_B + V_{interface} = V_{load}$

Relative Thickness is a Design Parameter

Resulting potential drop through each layer directly Impacts:

- Electrochemical performance
- Thermochemical stability
  - Pore formation -> Delamination
  - Tertiary phase formation

$$La_{1-y}Sr_yMnO_{3-\delta} + \delta ZrO_2 + \frac{3\delta}{2} O_O^{\times} \rightarrow La_{1-y-\delta}Sr_yMnO_{3-\delta} + \frac{\delta}{2} La_2Zr_2O_7 + \frac{3\delta}{2} V_O^{\bullet\bullet} + 3\delta e'$$

$$K \approx \left[La_2Zr_2O_7\right]^{\frac{\delta}{2}} \left[V_O^{\bullet\bullet}\right]^{\frac{3\delta}{2}} \left[e'\right]^{3\delta} = K_2 \left[La_2Zr_2O_7\right]^{\frac{\delta}{2}} P_{O_2}^{-\frac{3\delta}{4}}$$

EXTENSION OF CONTINUUM LEVEL ELECTROCHEMICAL MODEL TO THERMOCHEMICAL STABILITY: Electrolyte/Cathode Interface

Cathode Supported

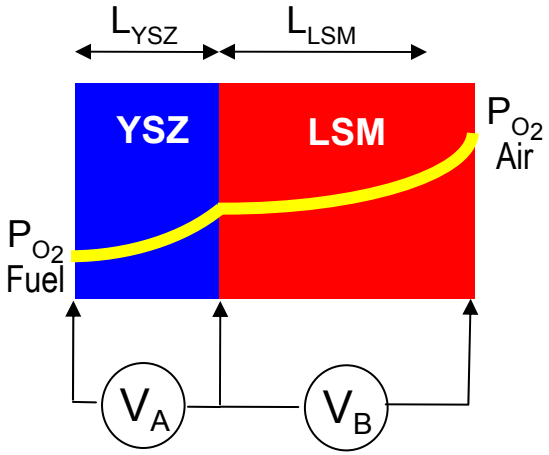

Anode or Electrolyte Supported

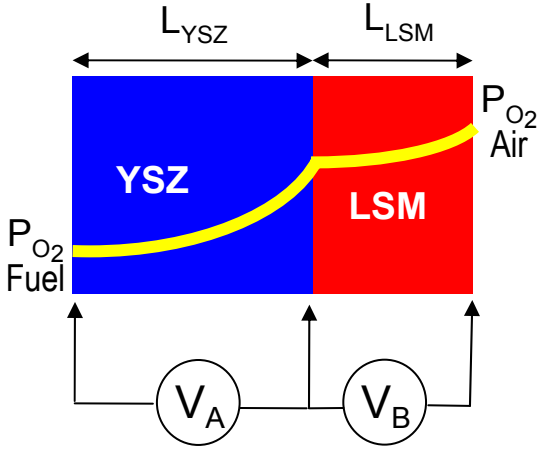

$$V_A + V_B + V_{interface} = V_{load}$$

Thickness ratio (L_{LSM}/L_{YSZ})

max-power

QuickTime™ and a TIFF (LZW) decompressor are needed to see this picture.

short-circuit

Modeled for dense cathode:
H_2/H_2O anode, air cathode,
800 °C; V_{oc} ~ 1.1 V

Voltage drop across LSM (V)

Cathode potential drop increases with:

- L_{LSM}/L_{YSZ}
- Current density

EXTENSION OF CONTINUUM LEVEL ELECTROCHEMICAL MODEL TO THERMOCHEMICAL STABILITY: Electrolyte/Cathode Interface

Cathode Supported

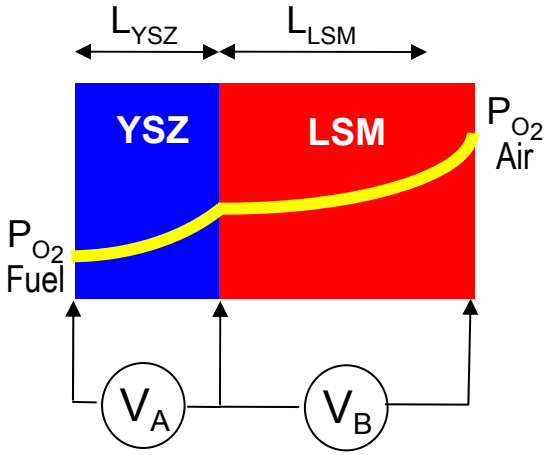

Anode or Electrolyte Supported

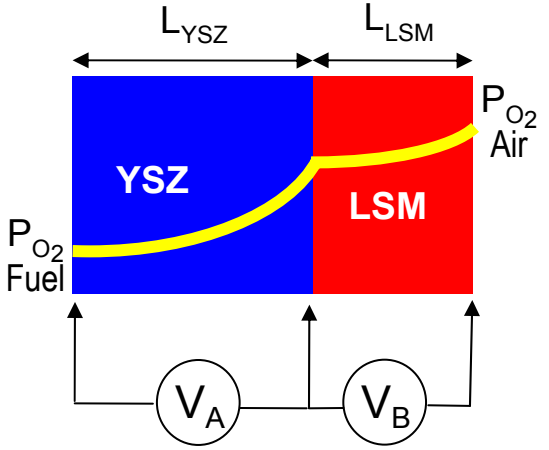

$$V_A + V_B + V_{interface} = V_{load}$$

- MIEC cathodes (LSF, LSC, etc.) will be included:
  - Will have greater potential drop due to ionic conductivity
- Effective of microstructure will be included:
  - Pore diffusion (e.g. Virkar, et al)
  - Grain boundary -space charge effects

TRANSIENT EFFECTS - Modeling

$R \equiv f(P_{O_2}, c_i, \Phi_{ext}, K)$

$C \equiv f(P_{O_2}, c_i, \Phi_{ext}, K)$

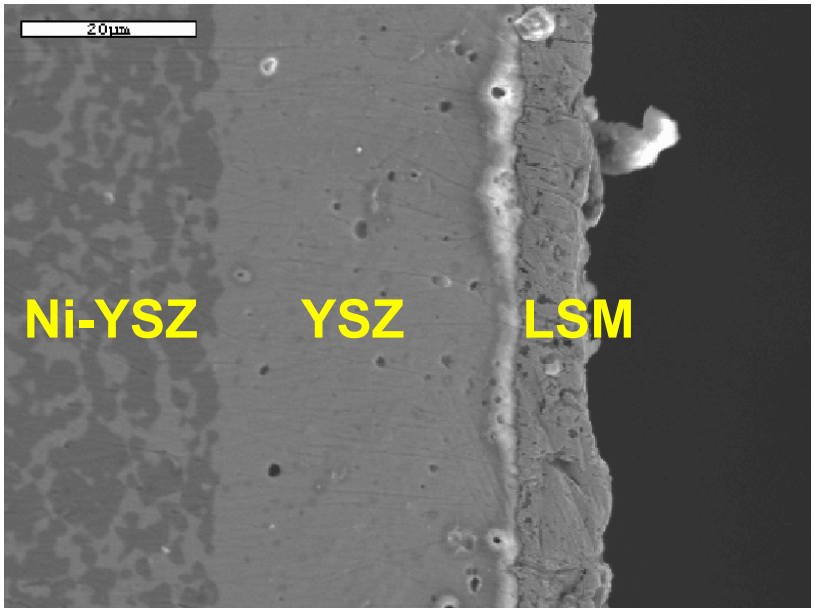

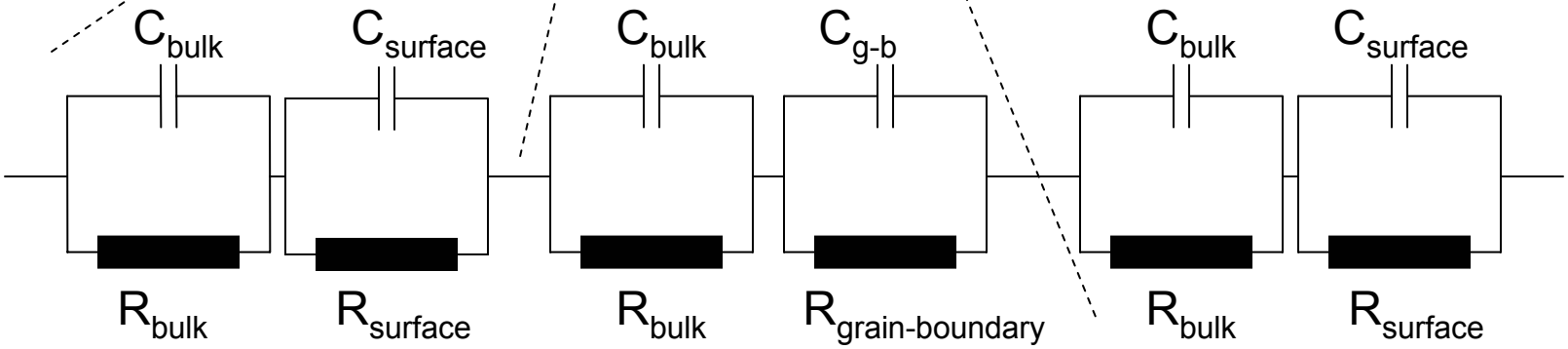

TRANSIENT TRANSPORT MODEL FOR ZIRCONIA

Nernst-Planck flux equation

$$j_i = -D_i \nabla c_i - u_i c_i \nabla \phi$$

Material balance equation

$$\frac{\partial c_i}{\partial t} = -\nabla j_i$$

Current equation

$$J = q \sum_i z_i j_i$$

Equations for flux, material balance, current and charge neutrality are manipulated to obtain expressions for the rate of change of defect concentration.

$$\frac{\partial c_V}{\partial t} = \frac{D_e D_V}{z_e D_e - z_V D_V} \left[(z_e - z_V) \nabla^2 c_V + z_e c_A \frac{q}{k_B T} \nabla^2 \phi \right]$$

$$\frac{\partial c_e}{\partial t} = \frac{D_e D_V}{z_e D_e - z_V D_V} \left[(z_e - z_V) \nabla^2 c_e + z_e z_V c_A \frac{q}{k_B T} \nabla^2 \phi \right]$$

And an expression for the electric field as a function of defect concentrations.

$$\nabla \phi = -\frac{J + \left(z_V q D_V \nabla c_V + z_e q D_e \nabla c_e \right)}{q \left(z_V u_V c_V + z_e u_e c_e \right)}$$

TRANSIENT EFFECTS ON DEFECT CONCENTRATION - using Fourier series

CASE 1: Introduction of a P_{O_2} gradient

Here we consider what happens when a zirconia electrolyte is first placed into a P_{O_2} gradient.

$$c_e(x,t) = \sum_{n=1}^{\infty} \frac{2\left((-1)^n c_{e,L}^{\infty} - c_{e,0}^{\infty} + c_e^0\right)}{n\pi} e^{-\alpha^2\left(\frac{n\pi}{L}\right)^2 t} \sin\frac{n\pi}{L}x + \frac{c_{e,L}^{\infty} - c_{e,0}^{\infty}}{L}x + c_{e,0}^{\infty}$$

$$\phi(x,t) = \frac{2D_e}{u_V c_A} \sum_{n=1}^{\infty} \frac{(-1)^n c_{e,L}^{\infty} - c_{e,0}^{\infty} + c_e^0}{n\pi} e^{-\alpha^2\left(\frac{n\pi}{L}\right)^2 t} \sin\frac{n\pi}{L}x + \frac{\phi_L^{\infty} - \phi_0^{\infty}}{L}x + \phi_0^{\infty}$$

CASE 2: Changing the load resistance and/the applied potential.

Here we consider what happens when the load resistance or an applied potential is changed for a zirconia electrolyte already operating in a P_{O_2} gradient

$$c_e(x,t) = \sum_{n=1}^{\infty} \frac{2\left[(-1)^{n-1}\left(c_{e,L}^0 - c_{e,L}^{\infty}\right) + \left(c_{e,0}^0 - c_{e,0}^{\infty}\right)\right]}{n\pi} e^{-\alpha^2\left(\frac{n\pi}{L}\right)^2 t} \sin\frac{n\pi}{L}x + \frac{c_{e,L}^{\infty} - c_{e,0}^{\infty}}{L}x + c_{e,0}^{\infty}$$

$$\phi(x,t) = \frac{D_e}{u_V c_A} c_e(x,t)$$

TRANSIENT EFFECTS ON DEFECT CONCENTRATION

CASE 1

Introduction of a P_{O_2} gradient

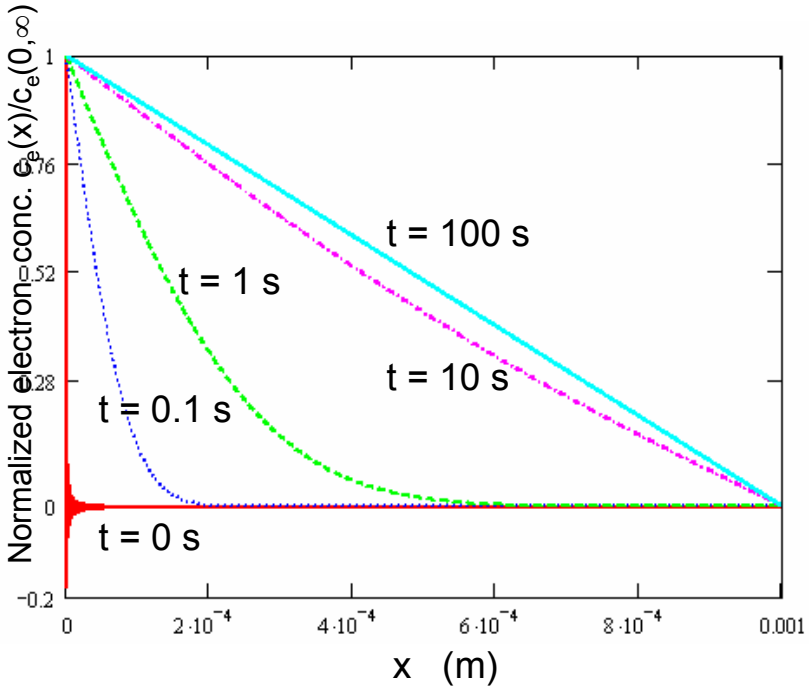

Before the zirconia electrolyte is introduced to a P_{O_2} gradient (i.e., at t = 0), the concentration distribution is flat. After the P_{O_2} gradient is introduced, a new concentration distribution gradually established.

CASE 2

Changing the P_{O_2} gradient/applied potential/load resistance

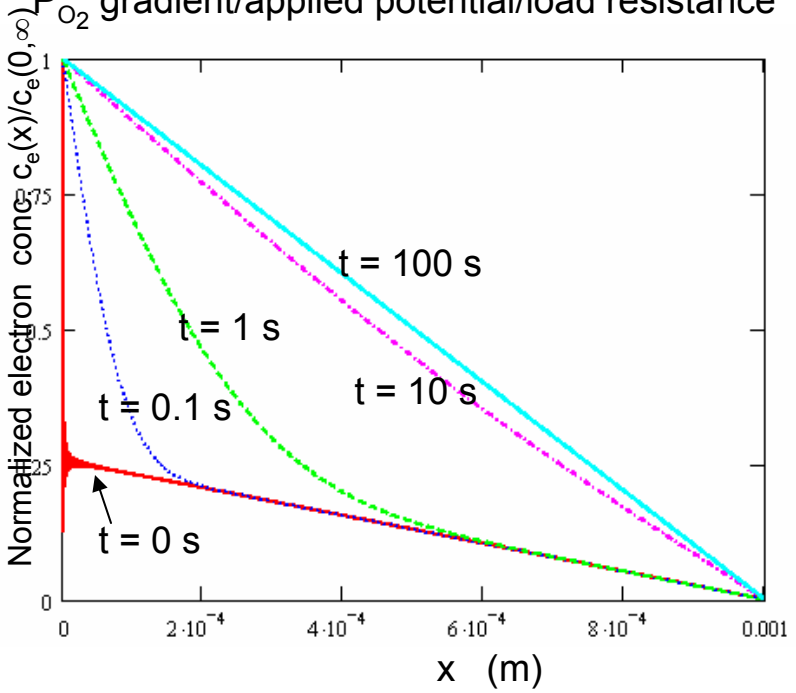

After the boundary concentrations are perturbed a new concentration distribution gradually established.

For the above processes, the time constant, τ,

- $\tau \propto 1/L$ (steady-state achieved more rapidly for thinner electrolytes)
- $\tau \propto D_e$ (rapid electron diffusion helps system to reach steady-state

TRANSIENT EFFECTS ON DEFECT CONCENTRATION

CASE 1 + Sinusoidal variation

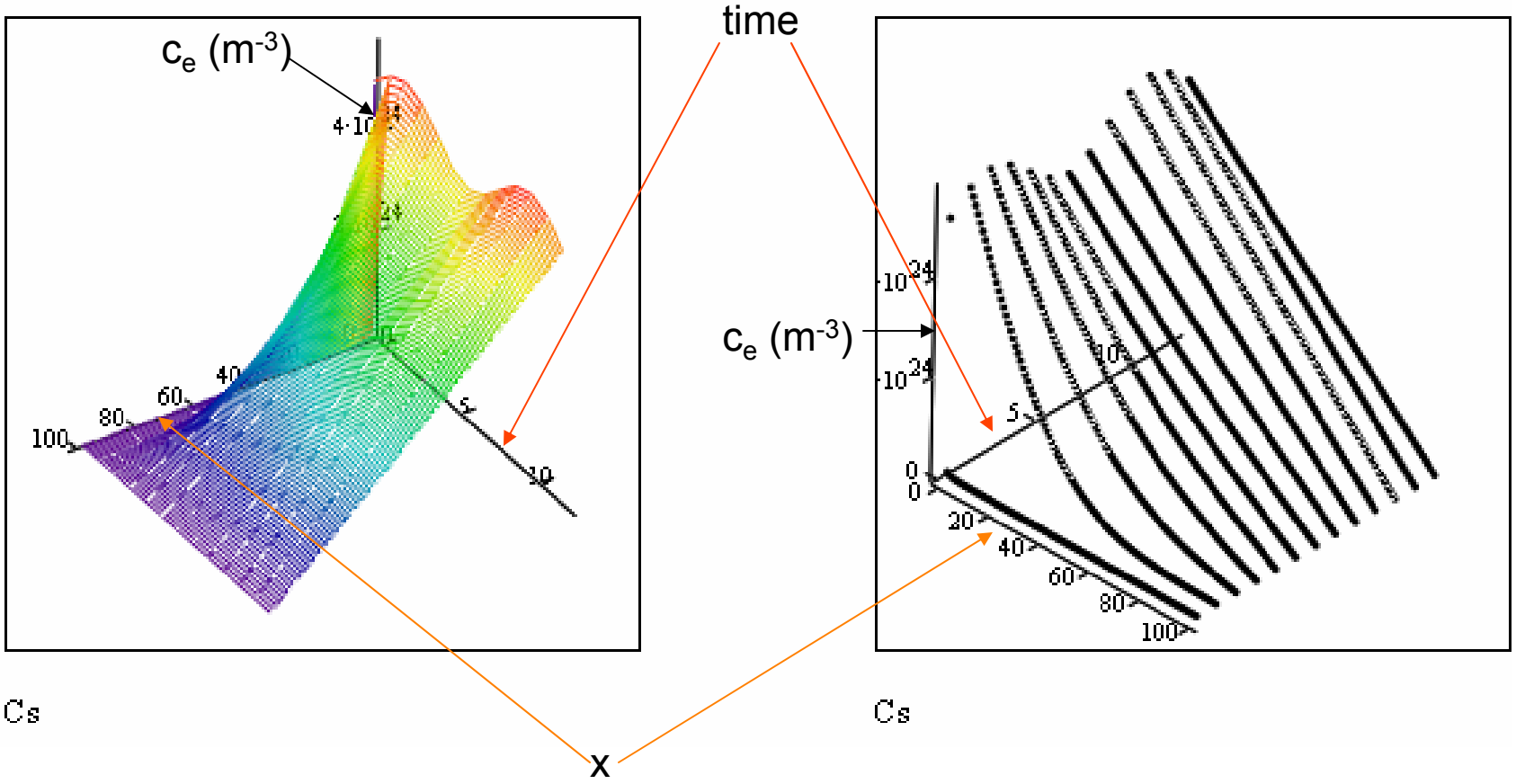

TRANSIENT EFFECTS ON DEFECT CONCENTRATION

CASE 2: Changing the P_{O_2} gradient/applied potential/load resistance

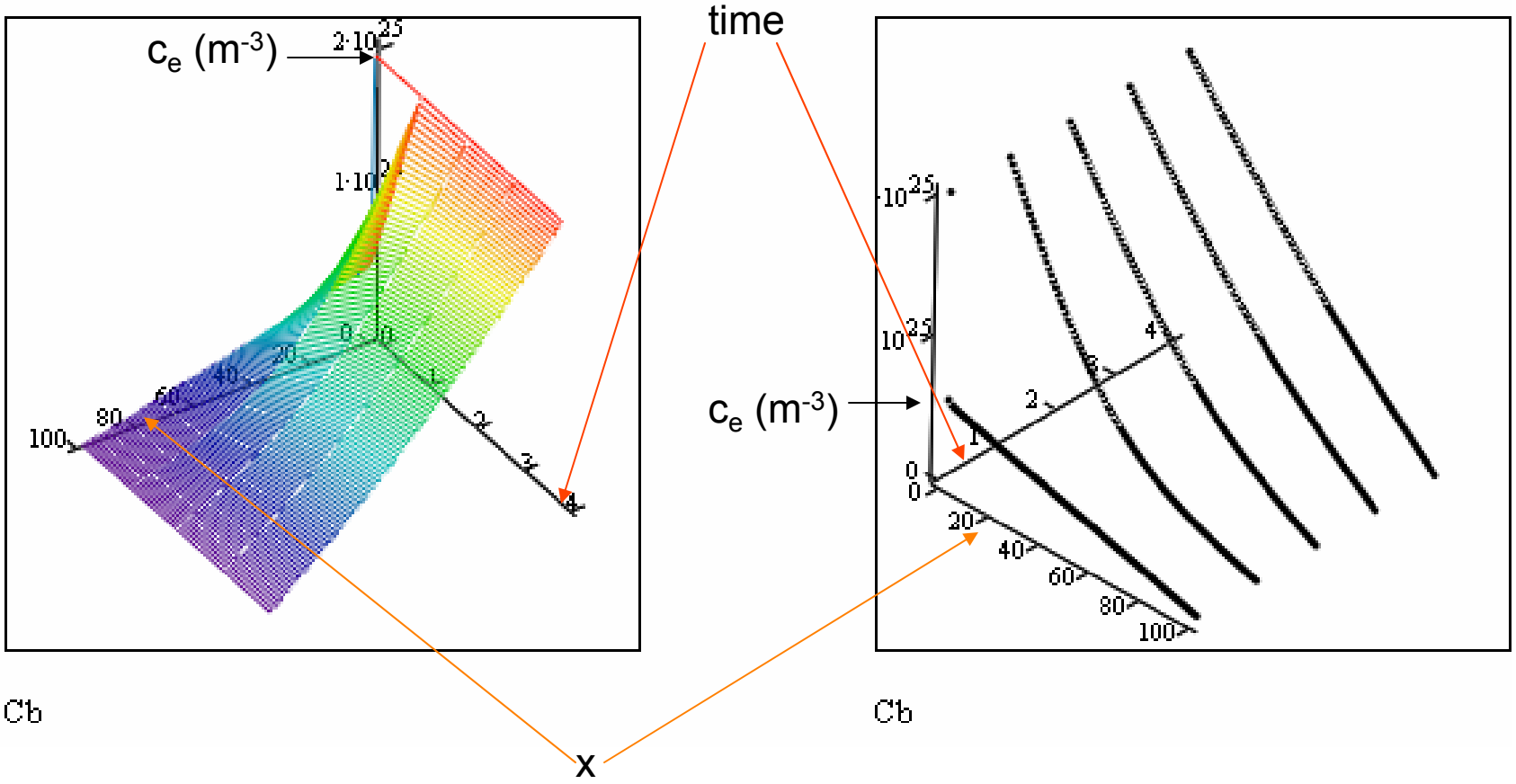

TRANSIENT EFFECTS ON DEFECT CONCENTRATION

CASE 2 + Square-wave variation

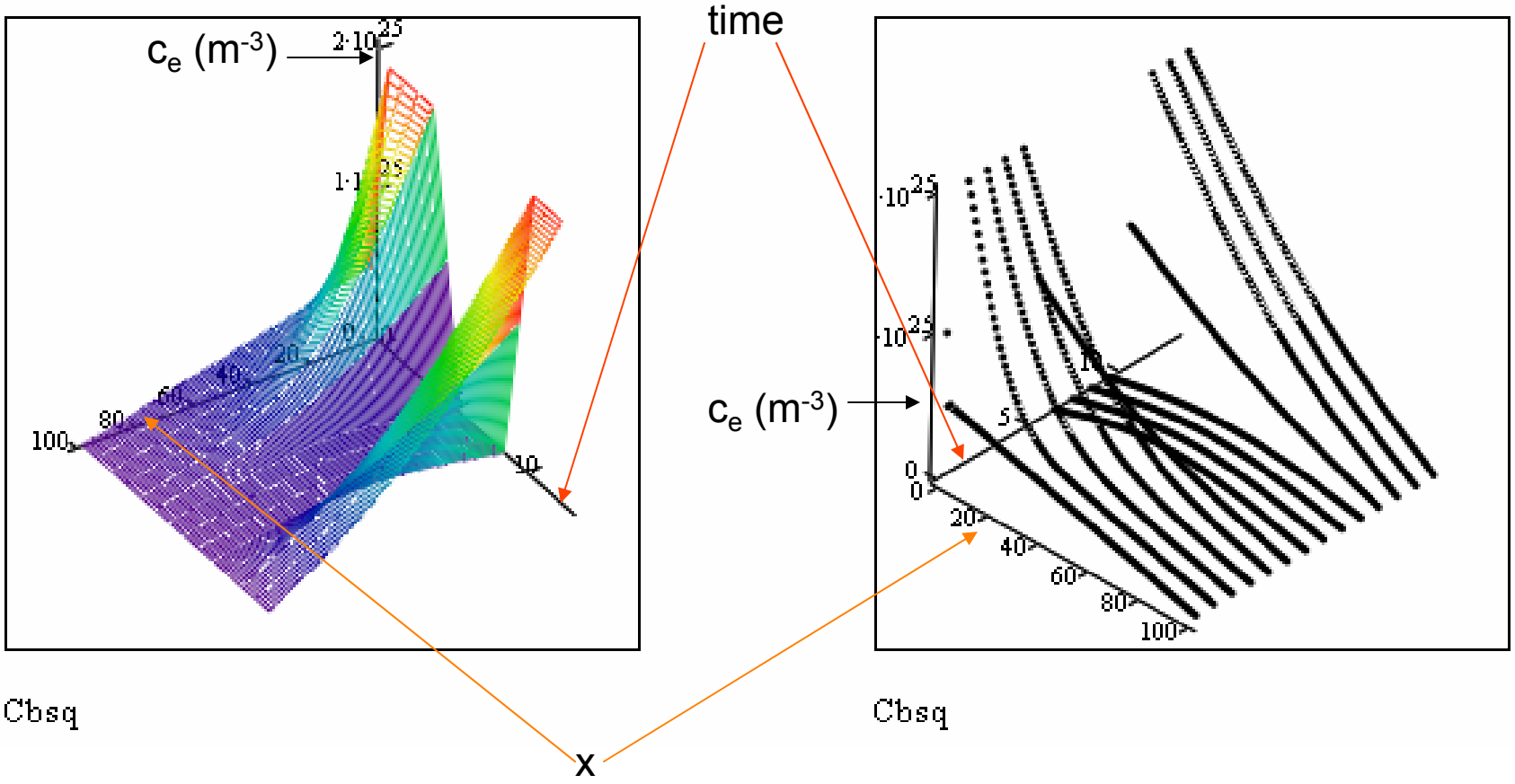

TRANSIENT EFFECTS ON DEFECT CONCENTRATION

Case 2 Changing the P_{O_2} gradient/applied potential/load resistance

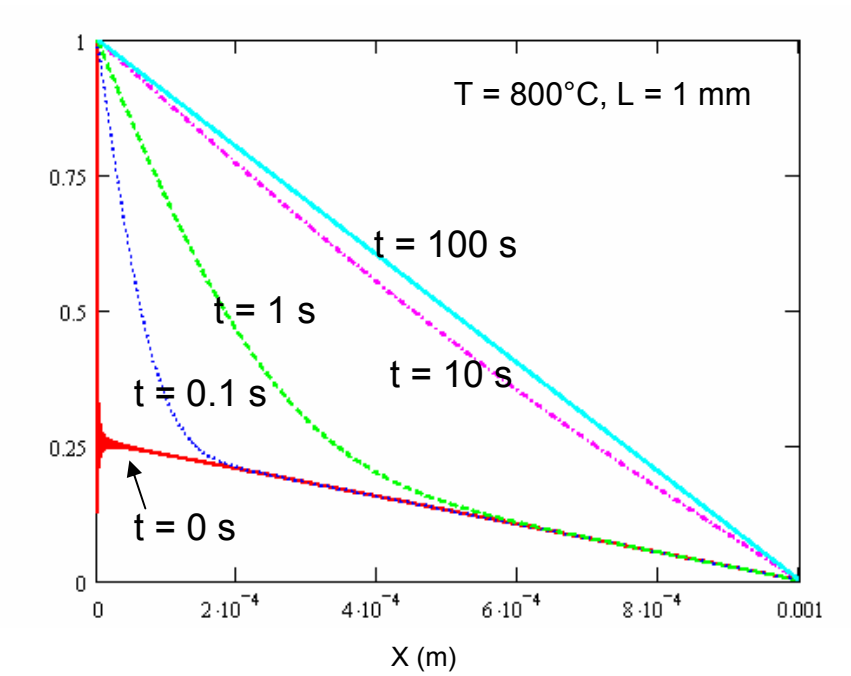

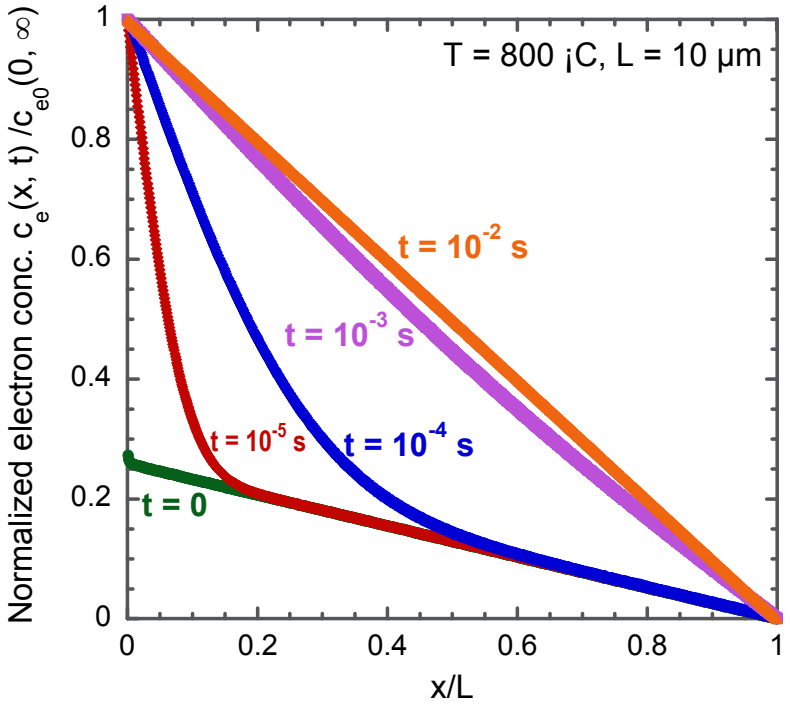

- Importance of transients depends on layer thickness

TRANSIENT EFFECTS - Experimental

$R \equiv f(P_{O_2}, c_i, \Phi_{ext}, K)$

$C \equiv f(P_{O_2}, c_i, \Phi_{ext}, K)$

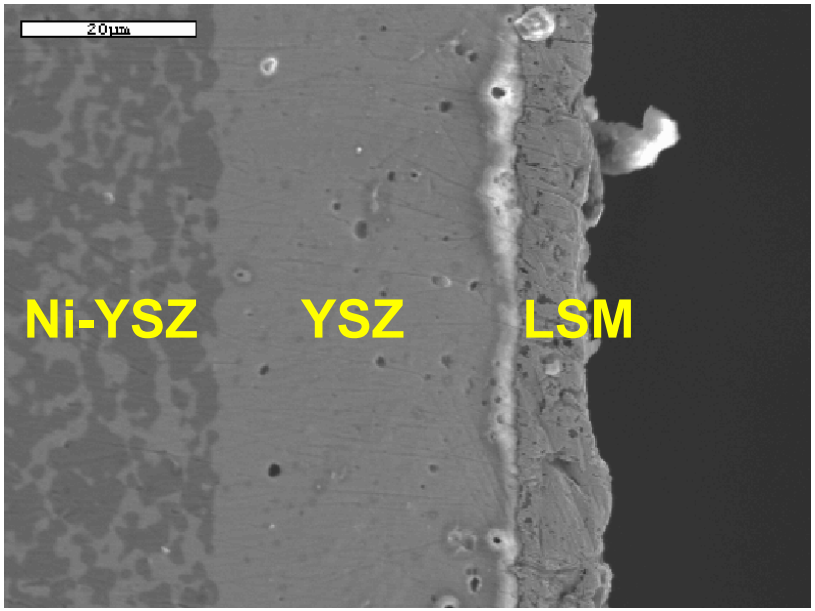

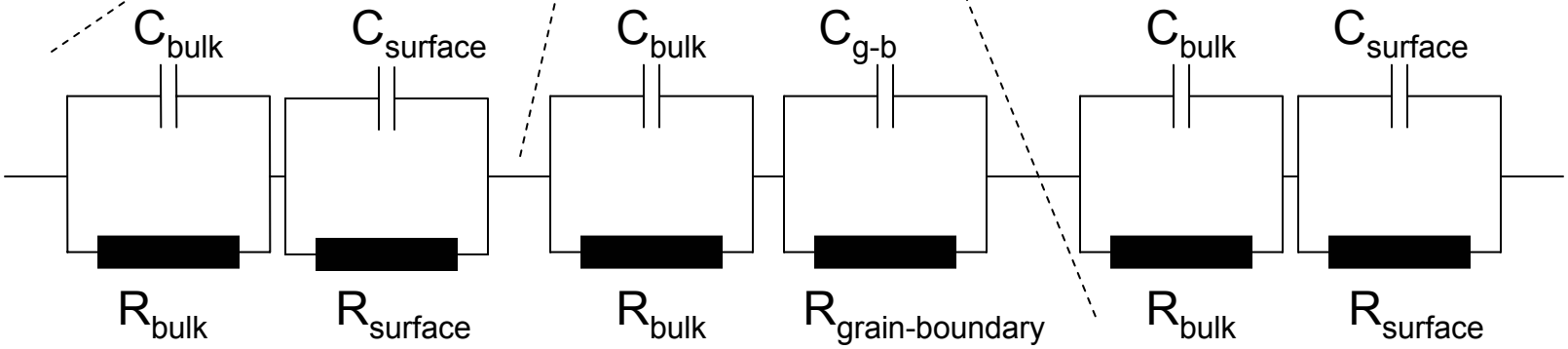

TRANSIENT TIME CONSTANTS

Table1. Electrode resistance, R, capacitance, C and time constant, τ ($=RC$) from EIS.

	Test Temperature (¡C)	$R_{electrode}$ (Ω)	$C_{electrode}$ (μF)	$\tau_{elecrode}$ (s)	$1/\tau_{elecrode}$ (Hz)
LSM/YSZ	500	50400	23.6	1.19	0.840
	700	820	51.5	4.22×10^{-2}	23.7
	800	131	71.2	1.02×10^{-2}	98.0
	900	22.1	115	2.54×10^{-3}	394
LSF/YSZ	700	438	208	9.11×10^{-2}	11.0
	800	134	165	2.21×10^{-2}	45.2
	900	1.24	11100	1.37×10^{-2}	73.0

- Choice of electrode material and operating temperature influence susceptibility to 60Hz transients

Samples supplied by NexTech

EFFECT OF ANNEAL on AC IMPEDANCE SPECTRA of LSM/YSZ/LSM CELLS

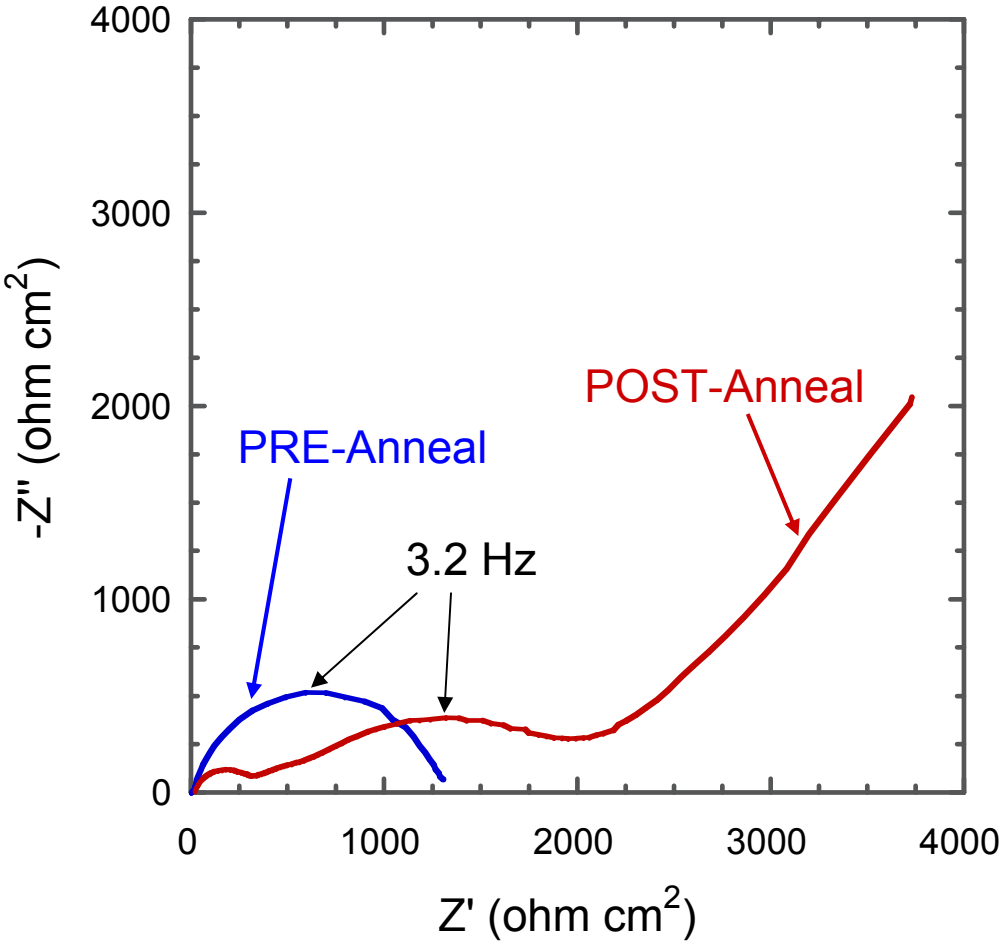

- Annealed at 1400 °C for 48 hours
- Presence of 3.2 Hz resonant frequency in pre- and post-anneal samples indicate that one transport phenomena remains the same
- Additional high frequency post-anneal feature due to formation of interfacial phase(s)
- Formation of additional phase to be compared with CLEM predictions of interfacial P_{O2}
- Time dependence of growth of additional phase to be compared with transient CLEM

Samples supplied by NexTech

Effect of Harsh Anneal on Microstructure at Interface

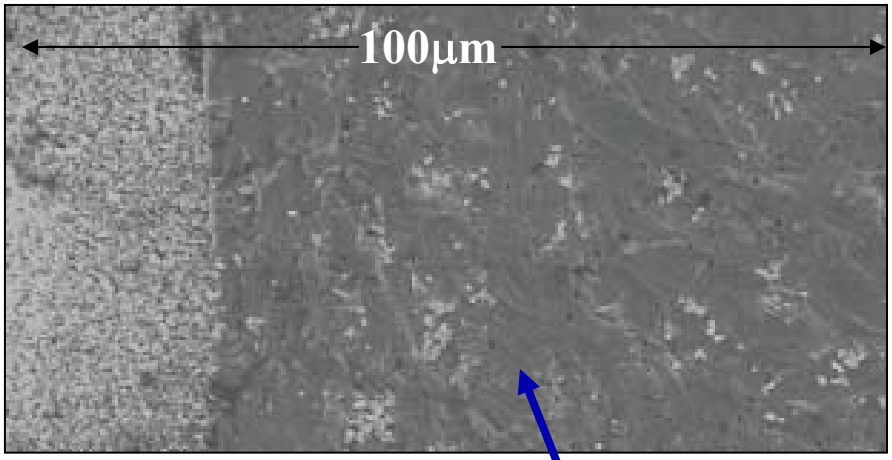

- LSM/YSZ interface **before** and **after** 1400ºC 48 hr anneal.

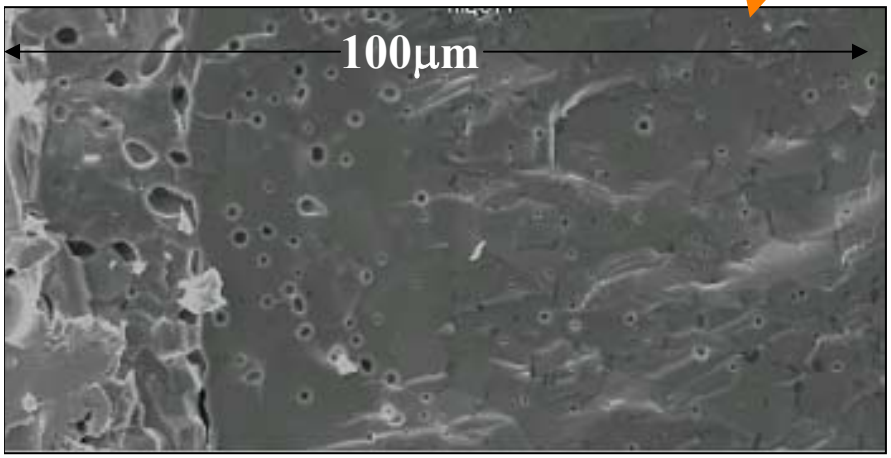

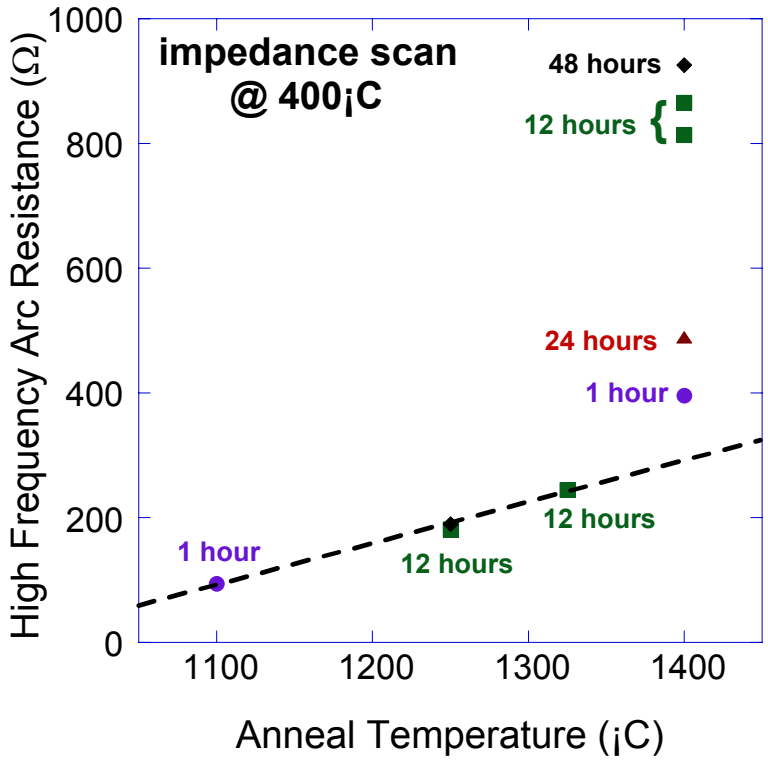

- We believe increase in high frequency impedance due to interfacial LZ formation

Samples supplied by NexTech

EFFECT OF APPLIED VOLTAGE on EIS SPECTRA of LSM/YSZ/LSM CELLS

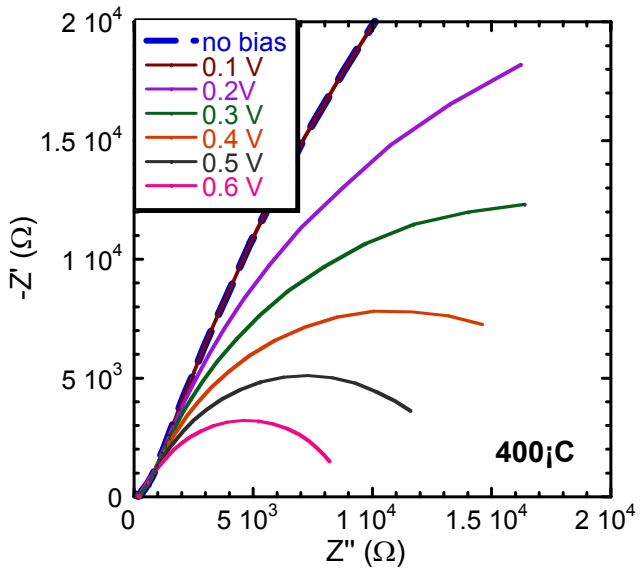

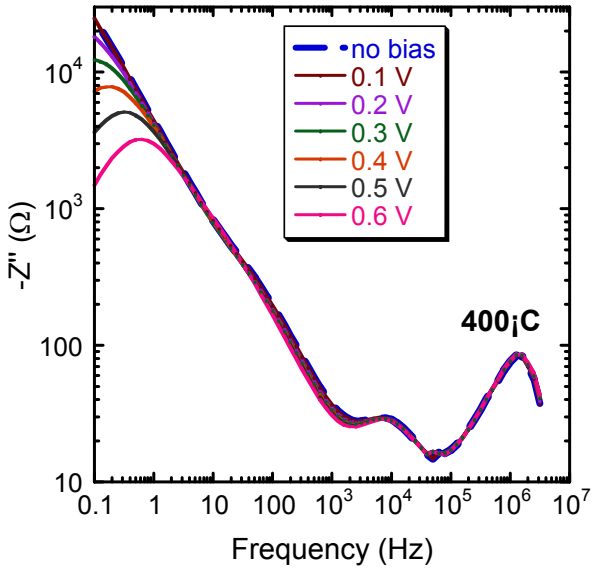

As the bias increases:

(a) The *low frequency* arc decreases in magnitude

(b) Only the *low frequency* process is affected significantly

Samples supplied by NexTech

EFFECT OF APPLIED VOLTAGE on EIS SPECTRA of LSM/YSZ/LSM CELLS

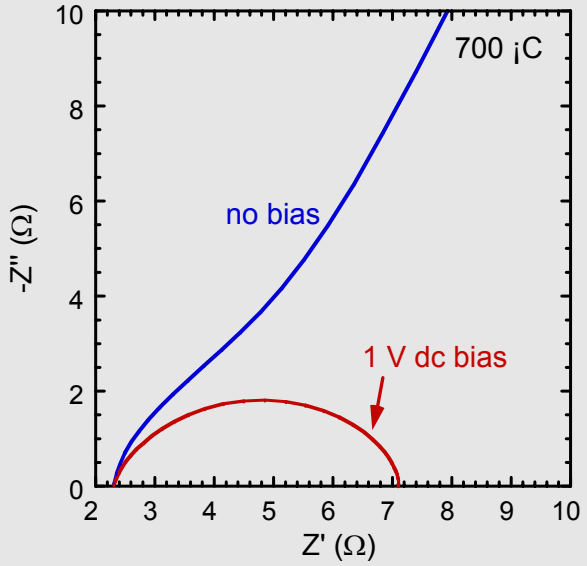

Application of 1 V d.c. bias removes the low frequency arc

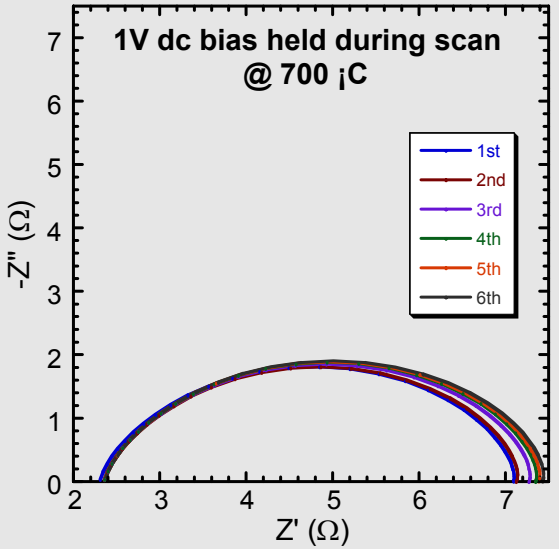

Steady application of 1 V d.c. bias followed by testing (**with** the bias present) shows slight growth of the high frequency arc

Transient application of 1 V d.c. bias followed by testing (**without** the bias present) shows **significant** growth of the low frequency arc

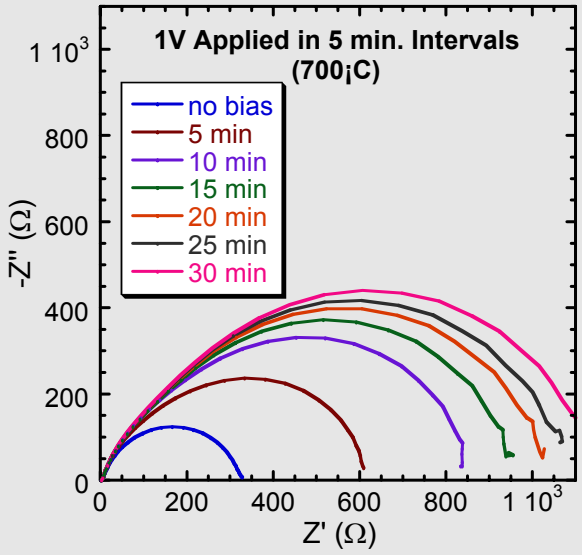

- Cathode or LSM/YSZ interface modified by application of voltage

Samples supplied by NexTech

EXTENSION OF CONTINUUM LEVEL ELECTROCHEMICAL MODEL TO THERMO-MECHANICAL PROPERTIES

$$E_{bond} \approx (1 - mn^{-1})Ba^{-m}$$

*where B, n and m are empirically determined constants and

a is the lattice parameter.

also

$$Y \sim a^{-(m+3)} \quad \text{and} \quad K_{IC} \sim Y^{1/2}a^{-3/2}$$

&

$$a \sim c_V$$

$$Y(x)/Y^{\circ} \approx \left(\sqrt[m+3]{Y^{\circ}}\, b_1 c_V(x) + 1\right)^{-(m+3)}$$

$$K_{IC}(x)/K_{IC}^{\circ} \approx \left(\sqrt[m+6]{\left(K_{IC}^{\circ}\right)^2}\, b_2 c_V(x) + 1\right)^{-\frac{m+6}{2}}$$

* M. Barsoum, in Fundamentals of Ceramics (McGraw-Hill, 1977).

SPATIAL VARIATION OF ELASTIC MODULUS (Y) & FRACTURE TOUGHNESS (K_{IC})

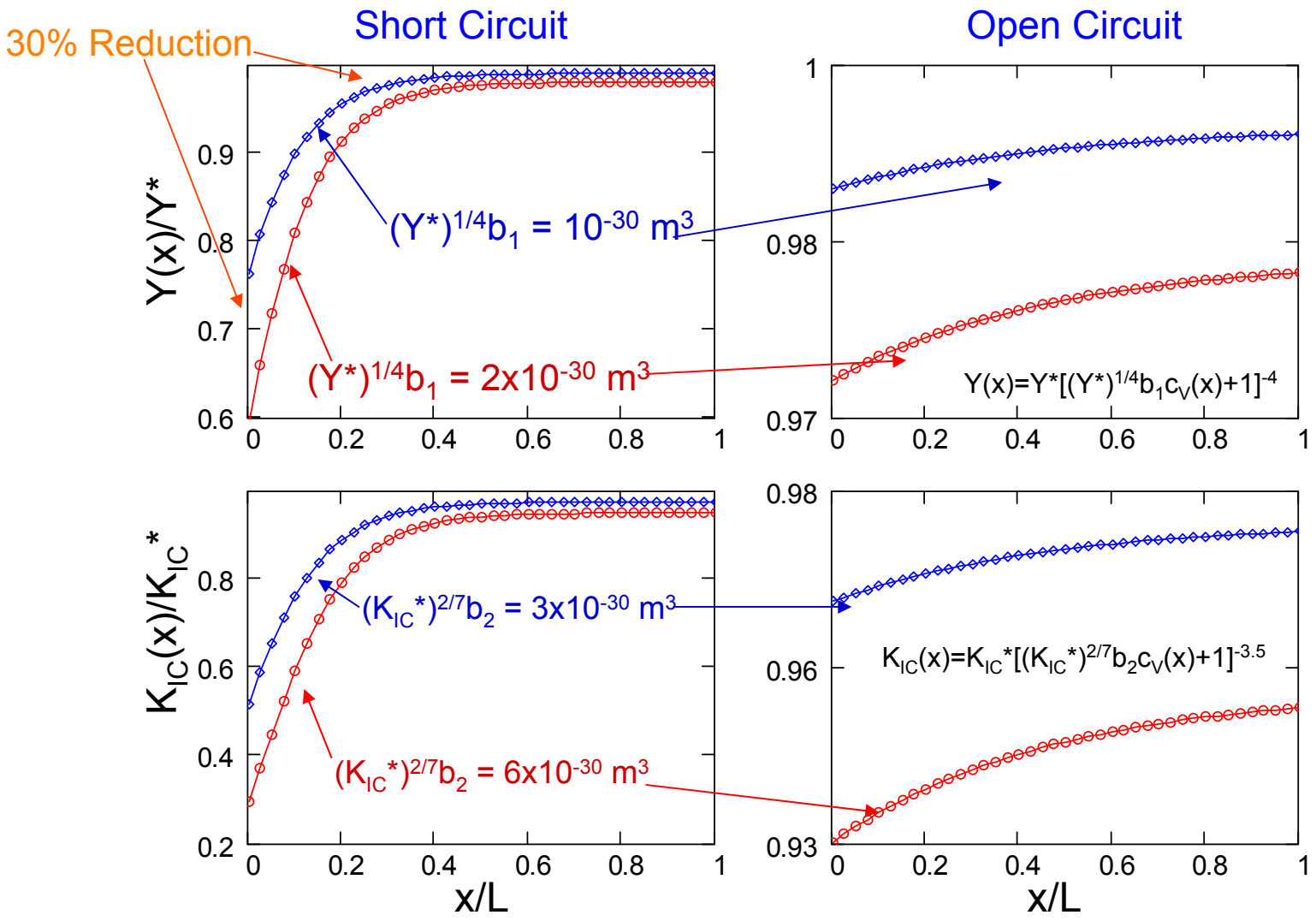

Indicates mechanical failure at anode under high current, consistent with LBL results*

*S. Visco, SECA, Albany, NY, Oct. 2003

THERMO-MECHANICAL PROPERTIES: EXPERIMENTAL WORK

- Vacancy concentration as a function of P_{O_2} (Cahn Microbalance)
  $c_v = f(T, P_{O_2})$ -> K(T)

- Thermal expansion as a function of P_{O_2} (THETA Dilatometer)
  $\Delta L \sim \Delta c_v = f(T, P_{O_2})$

- Bulk Elastic Moduli (Resonant Ultrasound) - E. Lara-Curzio, ORNL
  $Y \sim f(C_v) = f(T, P_{O_2})$

- Bulk Elastic Moduli and Fracture Toughness (Triboindenter)
  Y and $K_{IC} \sim f(C_v) = f(T, P_{O_2})$

- Elastic Moduli and Fracture Toughness of polycrystalline samples (MTS) at high temperature and as a function of P_{O_2}
  Y and $K_{IC} = f(T, P_{O_2}$, microstructure)

Initial Dilatometer Results

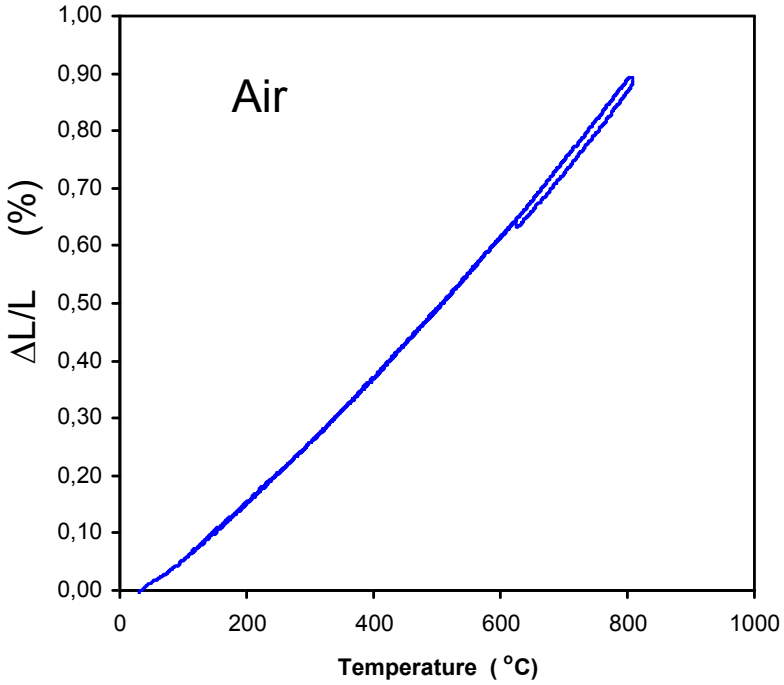

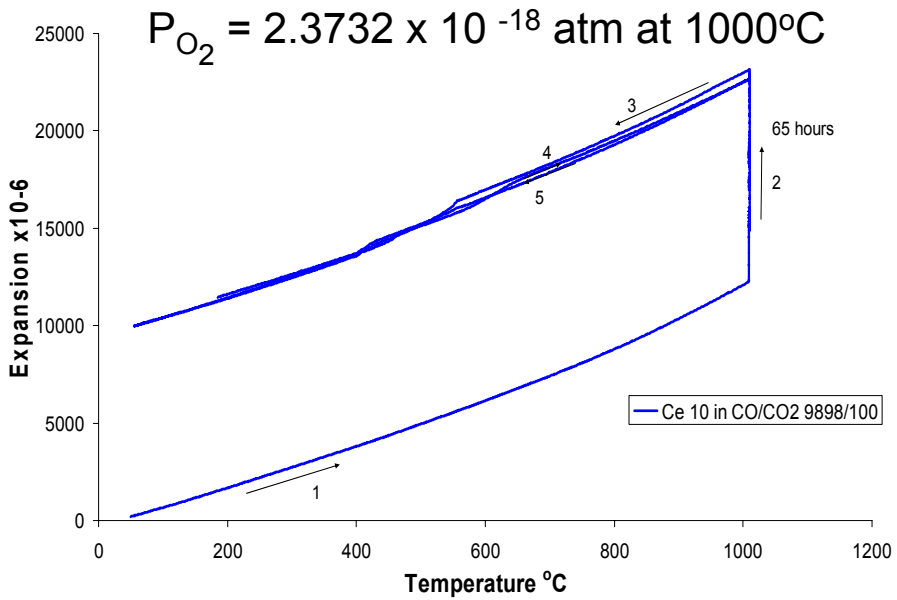

- Measured with Theta® dilatometer
- Initial length 12.1 mm CeO_2
- CTE / 10^{-6} $^oC^{-1}$

Temp	CTEx 10^{-6}
700°C	12.2 $^oC^{-1}$
750°C	12.7 $^oC^{-1}$
800°C	13.2 $^oC^{-1}$
800°C*	13.05 $^oC^{-1}$

*Sameshima *et al.* J.Cer. Soc. of Japan **110** (2002)

CeO_2- initial & reduced

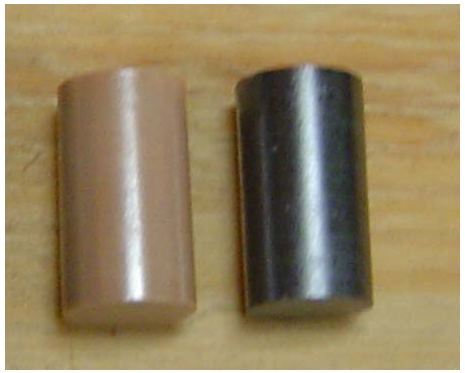

Bulk Elastic Moduli (Resonant Ultrasound) - E. Lara-Curzio, ORNL

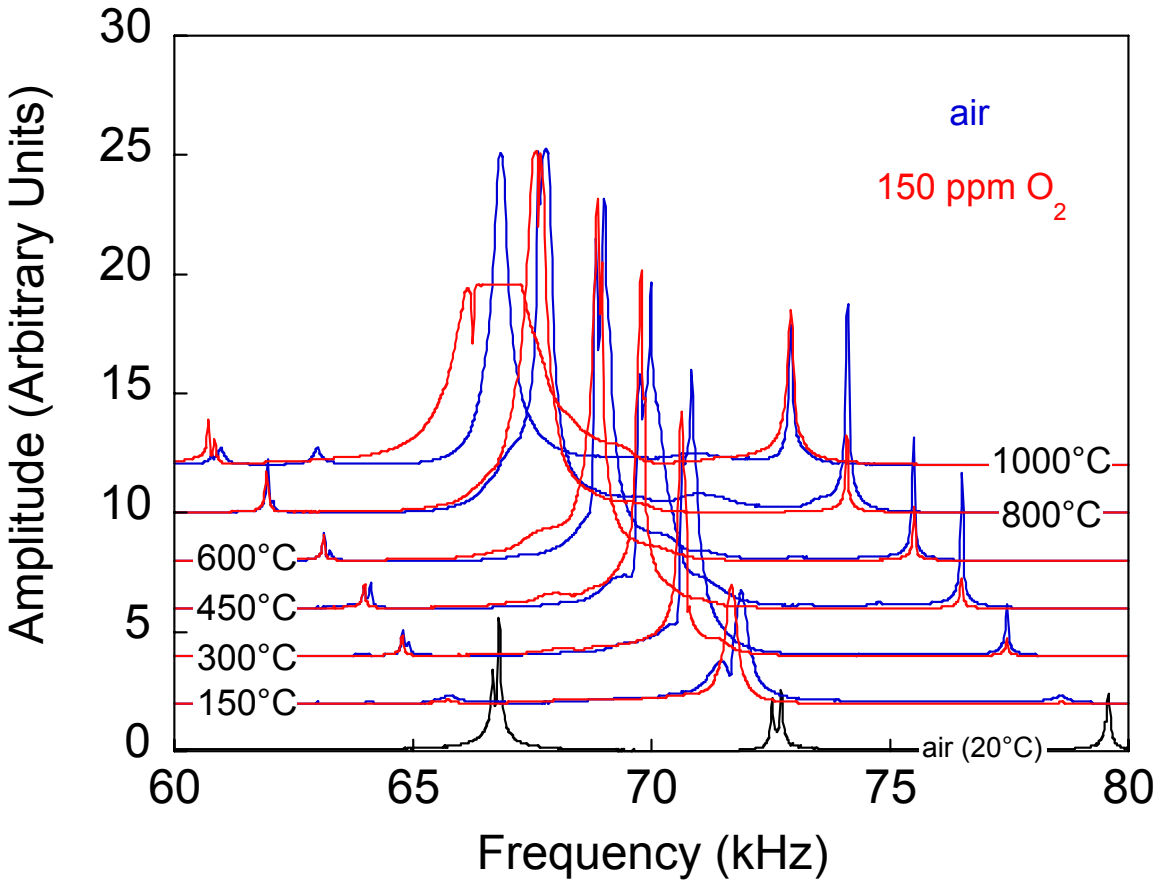

Broadening of peaks and shift to lower frequency indicate weaker bonds and lower modulus under low P_{O2}, consistent with model predictions.

$$Y \sim f(C_v) = f(T, P_{O_2})$$

Evolution of resonant ultrasound spectrum as a function of temperature for tests carried out in air (blue peaks) or in an environment with 150 ppm of O_2 (red peaks).

More than 40 peaks were used to estimate the magnitude of the elastic properties.

Evaluation of Mechanical Properties at Nanoscale

- Use electron Backscatter diffraction (EBSD) to generate crystal orientation map of specific grains

- Use Hysitron TriboIndenter to measure Elastic modulus (E) and Hardness (H) of selected single grain.

Hysitron TriboIndenter

(UF Major Analytical Instrumentation Center)

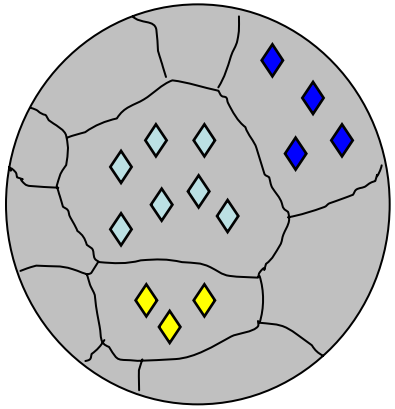

Effect of crystallographic orientation on elastic modulus and hardness evaluated statistically by applying many indents on grains of known orientation*

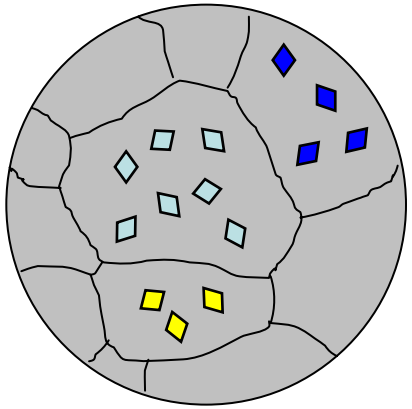

In-plane anisotropy measured by changing the indent orientation

*100 indents applied over 100 μm X 100 μm (~25 different grains)

Nano-indentation Test

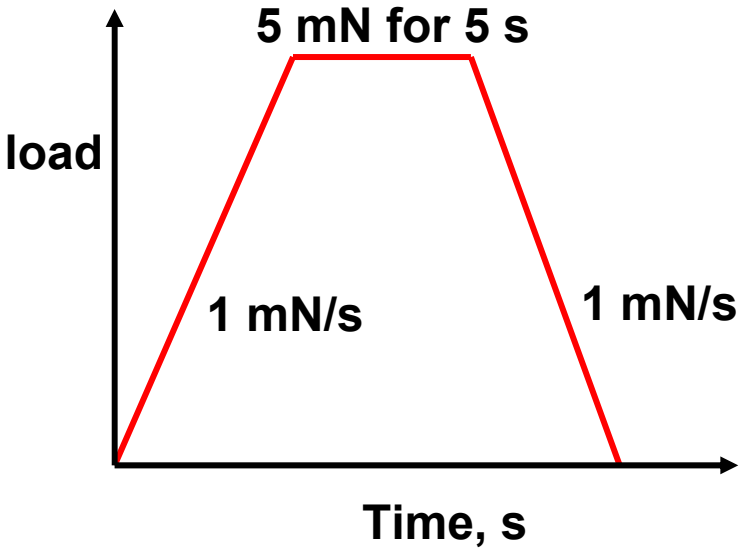

Load Function

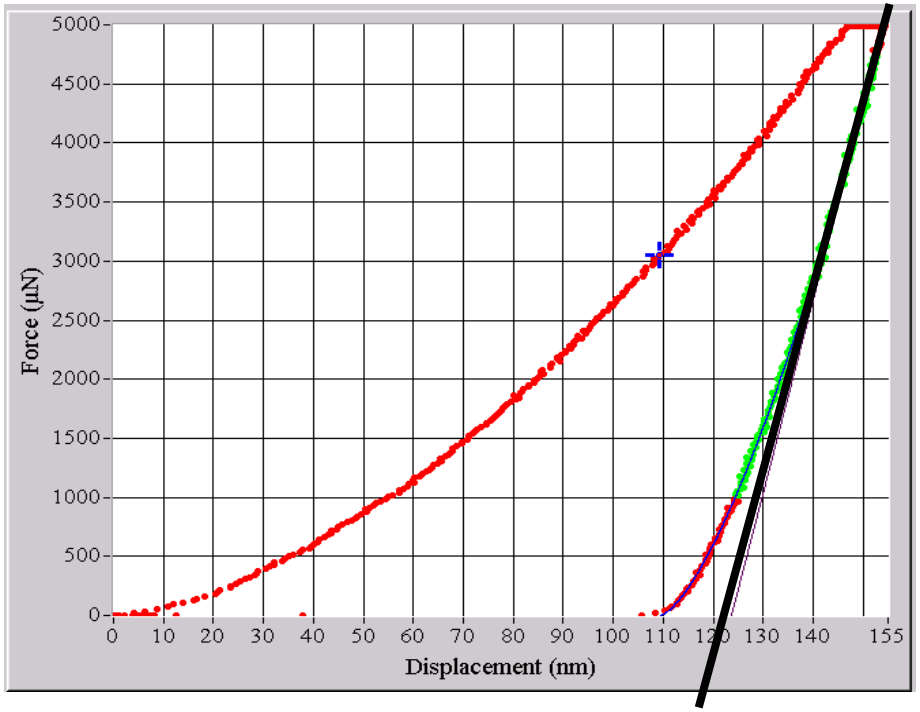

Reduced Modulus (Er) is calculated from the slope of the unloading segment

*100 indents applied over 100 µm X 100 µm (~25 different grains)

Nanoindent on Pure Ceria

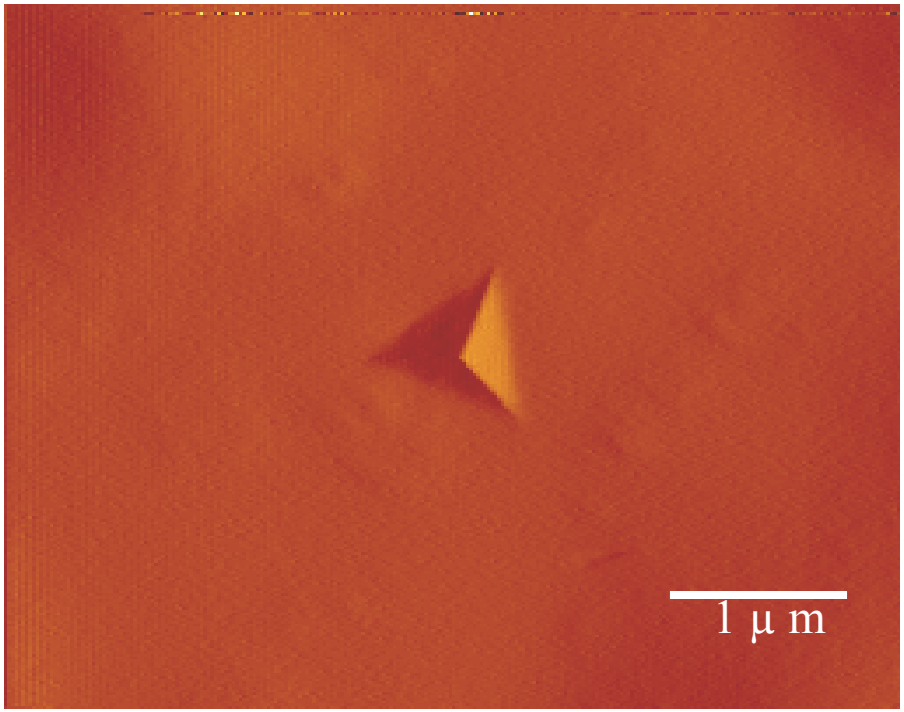

Nanoindents

Size: **~0.6 µm**

Depth: **~125 nm**

Specimen Preparation

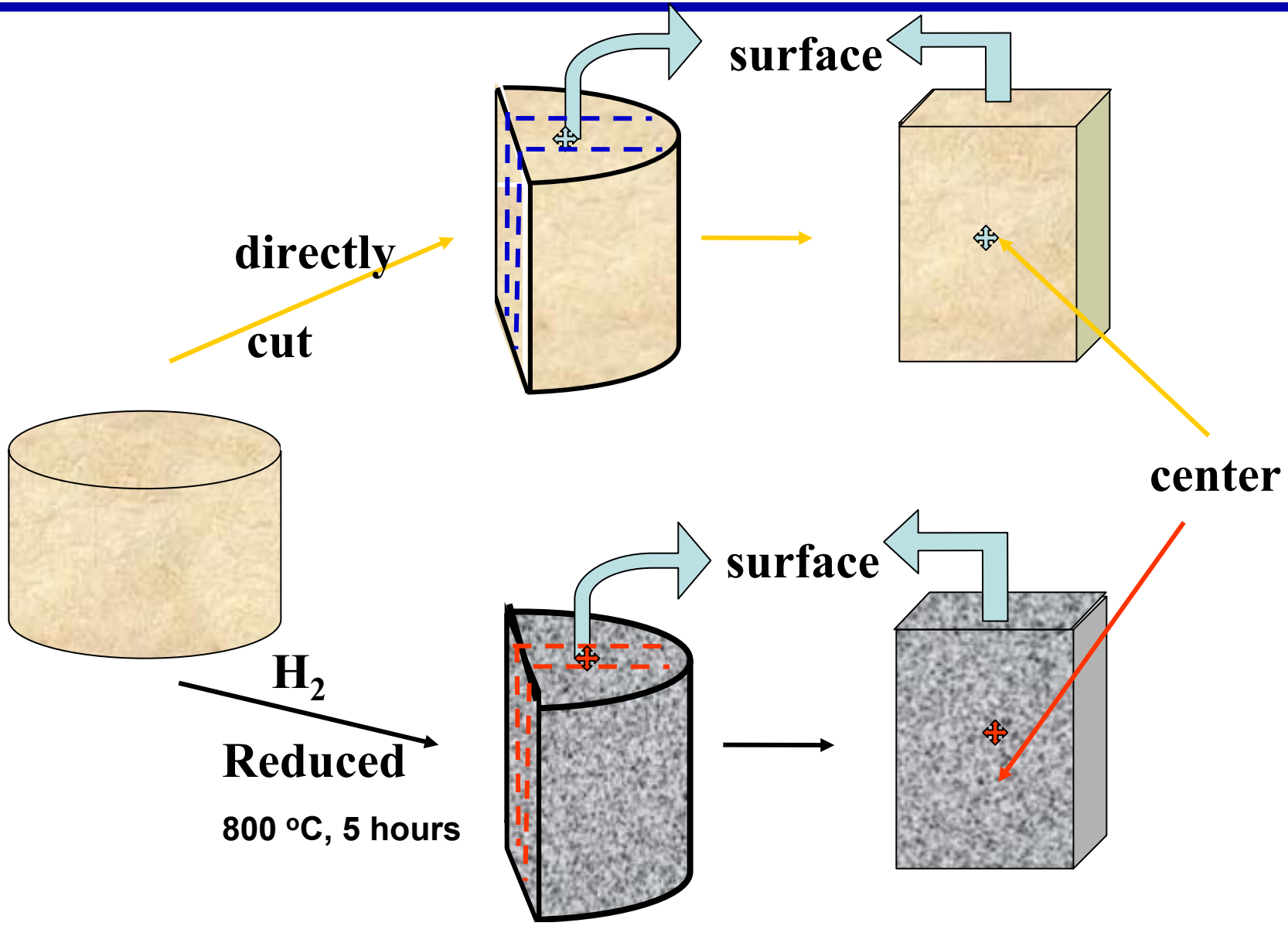

Inhomogeneous Structure of As-Sintered Sample

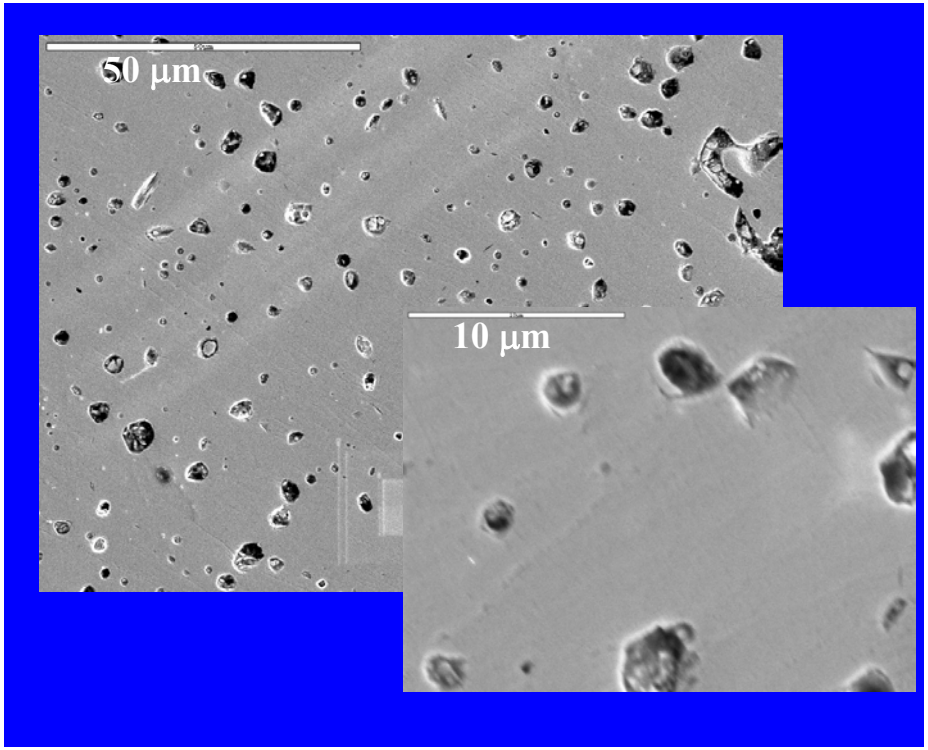

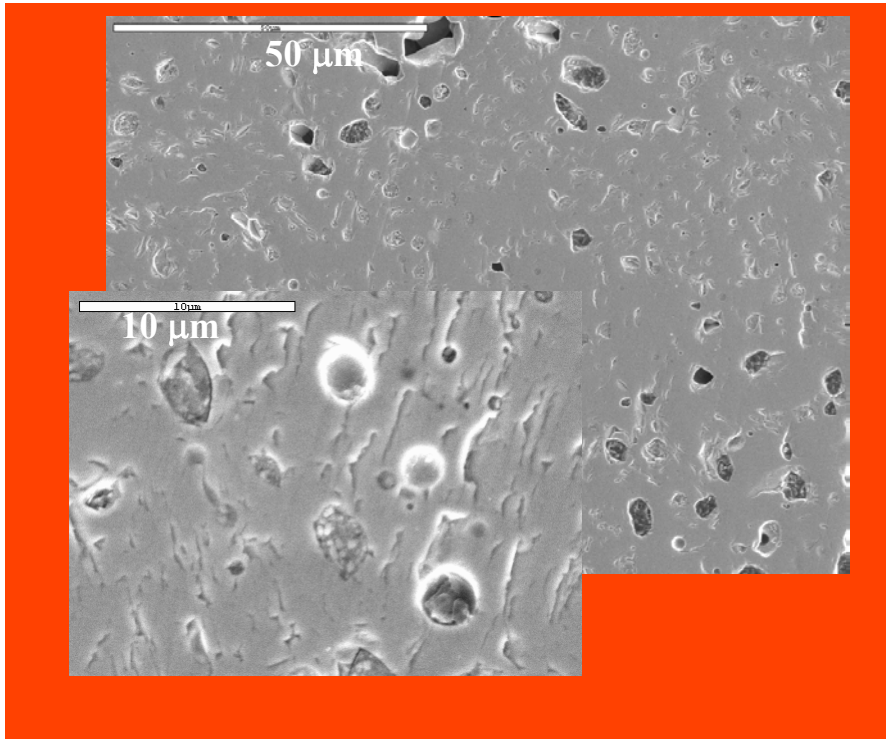

Surface

Modulus: 220.22 ± 7.08 GPa
Hardness: 9.52 ± 1.15 GPa

Center

Modulus: 187.46 ± 5.81 GPa
Hardness: 8.47 ± 0.69 GPa

•Lower modulus and hardness in center due to higher concentration of fine pores - microstructure.

Nanoindention Summary

		Modulus, E_r (GPa)	Hardness, H (GPa)
On the surface	As sintered	220.22 ± 7.08	9.52 ± 1.15
	H_2 reduced	148.87 ± 14.86	8.80 ± 1.41
	Reduction (%)	**32**	**7.6**
At the center	As sintered	187.46 ± 5.81	8.47 ± 0.69
	H_2 reduced	129.77 ± 13.04	7.31 ± 1.43
	Reduction (%)	**31**	**13.7**

- H_2 reduction decreased Modulus 30% regardless of microstructural differences
- Lower mechanical property values of the sample center due to higher fraction of submicron pores

Nanoindention Summary

		Modulus, E_r (GPa)	Hardness, H (GPa)
On the surface	As sintered	220.22 ± 7.08	9.52 ± 1.15
	H_2 reduced	148.87 ± 14.86	8.80 ± 1.41
	Reduction (%)	**32**	**7.6**
At the center	As sintered	187.46 ± 5.81	8.47 ± 0.69
	H_2 reduced	129.77 ± 13.04	7.31 ± 1.43
	Reduction (%)	**31**	**13.7**

- H_2 reduction decreased Modulus 30% regardless of microstructural differences
- Model predicted 30% reduction in Modulus

Elastic Moduli and Fracture Toughness (MTS) at High Temperature as a Function of P_{O_2}

For polycrystalline samples

Y and $K_{IC} \sim f(C_v) = f(T, P_{O_2})$

What is affect of microstructure?

Evaluation of Mechanical Properties at Micro-scale

MTS810 test machine

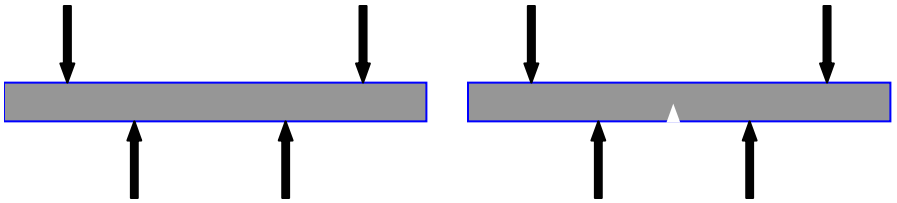

Four-point bending test using notched and smooth samples

- The MTS Testing system equipped with a vacuum furnace with controlled atmosphere allows mechanical testing to be conducted at high temperatures (up to 1600 °C) and under a variety of oxygen partial pressures.
- Four-point bending test will be used to measure E, M and K_{IC} of polycrystalline samples.
- Statistical analysis will be employed to ensure repeatable and reliable results.

Effect of Point Defects on Mechanical Properties

- **Objectives**
  - Verify the theoretical predictions.
  - Find out whether changes in the point defect concentration/type have significant impact on mechanical properties of typical SOFC components.
  - Evaluate elastic modulus (E), hardness (H), modulus of rupture (M) and fracture toughness (K_{IC}).
  - Evaluate intrinsic properties versus grain boundary and porosity effects.

- **Approach**
  - ✓ Obtain large-grained materials with various levels of defects by cooling samples, which have been equilibrated at elevated temperatures in a low P_{O_2} environment, fast to room temperature. Measure the mechanical properties as functions of crystallographic orientation for individual grains using an advanced nano-mechanical testing system.
  - ✓ Measure mechanical properties of bulk samples at high temperatures and low partial pressures of oxygen using a MTS system equipped with an environmental controlled furnace.

APPLICATION TO SECA TEAMS

- Developed spatial relationships that can be used to model:
  - Electrochemical performance
  - Interaction between materials
    - Phase instability ->performance degradation
  - Lattice expansion
    - Delamination
  - Mechanical properties
    - Mechanical failure

- Extended model to transient behavior to determine effect of:
  - Air/fuel compositional changes (start-up)and perturbations
  - Load changes
  - Thermal cycling

- Based on fundamental thermodynamic laws and constants:
  - Can be applied to any material set and geometry